AIAA JOURNAL
Vol. 46, No. 2, February 2008

Does a Model-Scale Nozzle Emit the Same Jet Noise as a Jet Engine?

K. Viswanathan*
The Boeing Company, Seattle, Washington 98124-2207

DOI: 10.2514/1.18019

A careful experimental study has been carried out to verify whether a model-scale nozzle produces the same jet noise as a jet engine, with the twin goals of 1) validating the practice of carrying out jet noise research at model scale for full-scale applications, and 2) aiding the identification of jet noise in measured total spectra from jet engines, which have contributions from several noise sources. A special test was carried out to measure pure jet noise from a low-bypass ratio jet engine at all the angles. Aeroacoustic measurements were made from model-scale nozzles at the Boeing Low-Speed Aeroacoustic Facility at the same operating conditions as the jet engine. Many issues that are pertinent for the comparison of scaled model data with engine data have been investigated thoroughly. These include the requirements of the instrumentation system for model and engine tests, suitable methodology for the calculation of the atmospheric attenuation coefficients, propagation effects, data repeatability, scaling of jet noise spectra, effects of the disparate Reynolds numbers and mixing perimeters between model nozzles and engines, etc. The data indicate that the weather corrections are accurate even at very high frequencies of interest in model tests. A new phenomenon of nonlinear propagation effects is identified for subsonic heated jets when the convective Mach number exceeds unity. The convective Mach number is shown to be a better indicator of nonlinear processes than high sound amplitudes, as has been believed in the past. As demonstrated, with the proper scaling factors, both narrowband and one-third-octave jet spectra can be collapsed. The concept of increasing the shear perimeter for achieving better mixing and hence reducing noise has no merit, even at supercritical pressure ratios. Excellent agreement between scaled model and engine spectra is demonstrated at all angles and frequencies for a variety of power levels; thus, it is possible to acquire high-quality spectra at high frequencies, provided proper care is taken. Finally, the major conclusion from the preceding results is that jet noise research carried out at model scale is applicable to jet engines.

I. Introduction

THERE are many noise sources in a jet engine: the jet, the inlet, the aft-fan, the turbine, and the combustor. Figure 1 shows a schematic sketch of a typical turbofan engine, along with the main noise sources and their principal directions of radiation. The inlet noise, consisting of the contributions from the fan and the compressor, peaks in the forward quadrant. In the aft directions, the jet and the aft-fan components are dominant. The combustor noise typically peaks at ∼110 to ∼120 deg from the inlet and the peak frequency is usually between ∼200 to ∼400 Hz. Most of these sources radiate noise over a wide range of frequencies of interest. This experimental study is concerned with a thorough investigation of several outstanding issues in jet noise, with the aim of clarifying long-held beliefs and aiding in the identification of jet noise in measured total spectra from jet engines. To achieve engine noise reduction, one must have a clear understanding of the different components of noise and their relative importance at various engine cycle conditions. Though a reduction in level for all the individual noise components is desirable, the practical overall benefit would be minimal unless the level of the dominant component (or the top two) is first reduced. The analysis of noise data from a static test of a jet engine, for example, requires the development of an "engine noise model," where the spectral shapes of the different engine components are extracted from the total measured noise spectra at all radiation angles. The first step in this process usually involves the subtraction of the jet noise, estimated by either a prediction method or the extrapolation of model-scale data, with the remaining noise bookkept as turbomachinery noise. The turbomachinery noise is then broken down into fan noise, turbine noise, combustor noise, etc., subsequently. This entire process of source decomposition is somewhat subjective necessarily, as there is no accurate way of determining/predicting the levels of the individual components at a given operating condition and for a given geometry. Proprietary methods are used by the aircraft manufacturers and engine companies to accomplish the source decomposition. As can be appreciated, this procedure is an art and a science and requires considerable experience and judgment. Though empirical, the prediction methodology for jet noise is the most well established and therefore constitutes the first step in the development of a component model for engine noise. This prevailing procedure leads to the following important question: does a scale-model nozzle produce the same jet noise as a jet engine?

First, let us examine the noise spectra from an engine at three different radiation angles of 90, 120, and 150 deg in Fig. 2a. The origin of the coordinate system is located at the center of the nozzle exit plane and on the engine axis, which is at the center of the primary nozzle. The polar angles are measured from the jet inlet axis, with the jet exhaust axis corresponding to 180 deg. These spectra are from a commercial high-bypass ratio turbofan engine at typical takeoff power, with a bypass ratio (BPR) of ∼5, and measured from a static engine test. We note that as we move to aft angles, the spectral level at the lower frequencies keeps increasing and the peak moves to lower frequencies; these are characteristic features of jet noise and one can identify the jet noise component as being dominant at the lower frequency regime. However, at the higher frequencies ($f \geq 1000$ Hz) the spectral level at a radiation angle of 90 deg, for example, keeps increasing and is clearly dominated by the turbomachinery noise. Figure 2b shows a component model for the spectrum at 90 deg for this high takeoff power; the jet and the aft-fan components along with the measured spectrum are shown. The tones at the lower frequencies are from other components. These two figures illustrate the process involved in the extraction of the

Presented as Paper 2936 at the 11th AIAA/CEAS Aeroacoustics Conference, Monterey, CA, 23–25 May 2005; received 4 June 2005; revision received 20 July 2007; accepted for publication 2 August 2007.

*Mail Stop 67-ML, Post Office Box 3707; k.viswanathan@boeing.com. Associate Fellow AIAA.

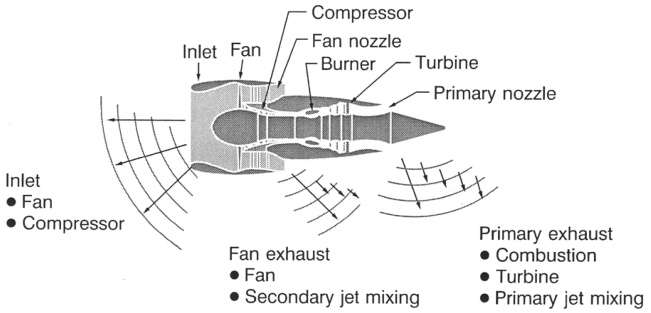

Fig. 1 Cutaway drawing of a typical turbofan engine with the different noise sources. The principal noise radiation directions are also shown.

individual spectral shapes. Note that, whereas it is possible to measure pure jet noise with a well-controlled experimental setup and a jet rig fed by compressed air with no turbomachinery, there is no easy way of measuring the aft-fan component directly. Given that

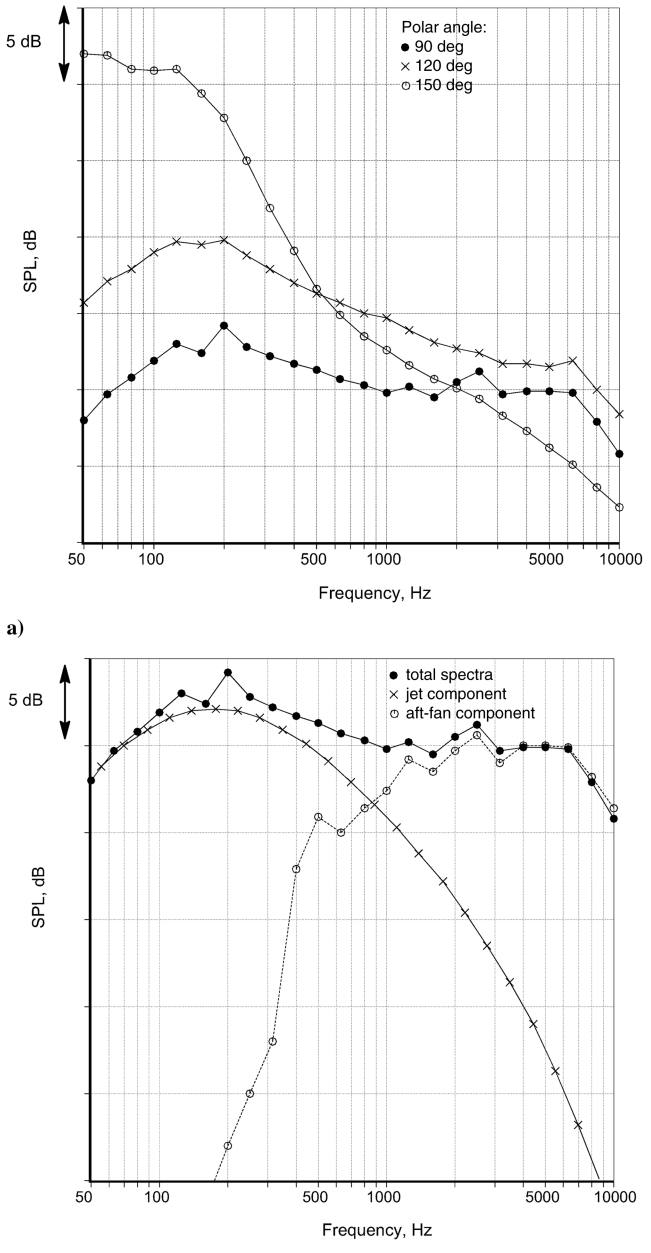

Fig. 2 Spectra from a high-bypass ratio turbofan engine. High takeoff power. a) Typical measured spectra, b) breakdown of measured spectra at 90 deg into individual components.

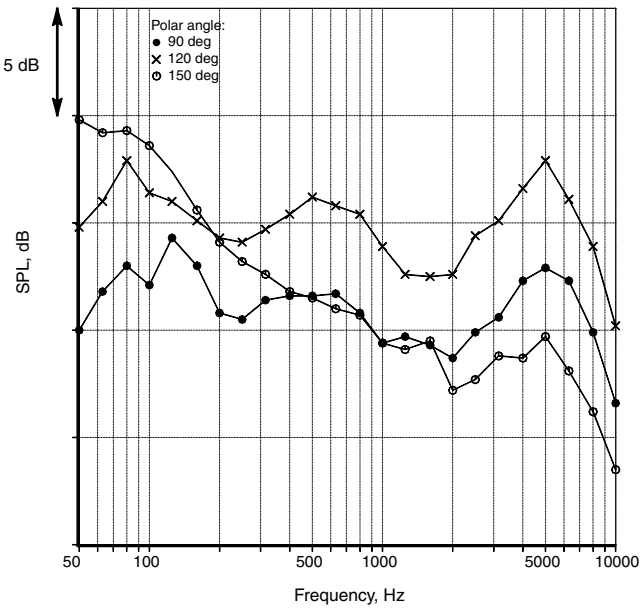

Fig. 3 Typical measured spectra from a high-bypass ratio turbofan engine. Lower power.

there is no accurate prediction method for the spectra for aft-fan noise, one has to take recourse to the aforementioned procedure of subtracting the jet noise from the total to obtain the aft-fan component. It should be clearly recognized that this entire process is complex and that one cannot know the exact levels with certainty.

Figure 3 shows spectra at the same angles, but at a lower power. It is immediately evident that the extraction process is not as clear-cut as at high takeoff power and the complexity of this task increases multifold. It is all the more important then to have a validated method for the identification of the jet and turbomachinery noise. These three figures highlight the need for an accurate database and prediction methodology for jet noise, especially over a wide range of jet velocities and for realistic geometries of the engine exhaust systems. As noted earlier, most of the prediction methodologies for jet noise used by the industry are empirical in nature and hence are only as good as the databases on which they are based. Viswanathan [1,2] noted that variations in experimental techniques, quality of the jet rig and measurement systems, anechoicity of the test chamber, processing, analysis, and interpretation of spectra, and a few other factors have contributed to the prevailing confusion about some characteristics of jet noise. An examination of the data obtained at various jet noise laboratories, and reported in the preceding two references, indicated that most of the spectra are contaminated by extraneous noise sources and are unsuitable for scientific and engineering applications. This is especially so for the development, validation, and extension of prediction methods and for the important goal of achieving noise reduction, where reliable and repeatable data are imperative.

It is clear from the engine noise spectra shown before that it would be impossible to assess whether a model-scale nozzle indeed generates the same level of jet noise, because the turbomachinery noise is significant over a wide range of frequencies. Recall that the preceding description of noise is for a high-BPR turbofan engine. However, the balance of noise sources is vastly different for a turbojet or a very low-BPR turbofan engine. For these types of engines, the jet noise component is the single dominant source, especially at high power, and the importance of the turbomachinery noise is greatly diminished. Hence, a high-BPR turbofan engine is not the right choice for addressing the fundamental question posed earlier and a turbojet or a low-BPR turbofan engine is required. Further, particular consideration must be given to the reduction of the noise from the other components as much as possible. The inlet noise is dominant in the forward angles, especially because the level of jet noise is low. Therefore, the measurement of pure jet noise in the forward quadrant presents a formidable challenge. A special test was

carried out to measure pure jet noise at all angles. Good model-scale data were also acquired at the same cycle conditions. Details of the test programs are given; issues that must be addressed in the measurement and scaling of the data are enumerated and evaluated in the following sections. Finally, comparisons of data from the model-scale nozzles and two jet engines are presented.

II. Details of the Test Programs

A. Engine Test

A low-bypass ratio turbofan engine with BPR $\cong$ 0.30 was chosen as the candidate engine. Several measures that would enhance the measurement of pure jet noise at all angles were taken. Figure 4 shows a schematic of the test setup; a treated inlet duct was incorporated upstream of the engine to minimize inlet noise. The inlet duct was preceded by a very long duct with a length of 100 ft; this long duct served the dual purpose of preventing the reingestion of the hot exhaust gas, as well as eliminating/minimizing the radiation of the inlet noise to the microphones at the lower polar angles. An acoustically treated spool piece was added to the back of the engine, downstream of the turbine, to minimize turbine noise and the aft-radiating component of fan noise. Given the low-BPR and the small size of the fan, the aft-fan component is not expected to be significant for this engine. Finally, long nozzles of different designs were attached to the downstream-end of the spool duct and aeroacoustic measurements were made at different cycle conditions.

B. Model-Scale Test

A comprehensive experimental program has been carried out at the Low-Speed Aeroacoustic Facility (LSAF) at Boeing over the past few years. Detailed descriptions of the test facility, the jet simulator, the data acquisition and reduction process, etc., may be found in Viswanathan [1]. Figures 1a and 1b in [1] provide a schematic sketch of the anechoic facility and the jet rig, with the layout of the microphones also included. Therefore, only an overview of the tests is provided here. The jet simulator is embedded in an open-jet wind tunnel, which can provide a maximum freestream Mach number of 0.32. Both acoustic and thrust measurements were made simultaneously. Typically, several microphone arrays at different azimuthal angles were used. The microphones were at a constant sideline distance of 15 ft (4.572 m) from the jet axis, except the microphone at 155 deg, which was at a distance of 12.75 ft (3.886 m). All angles are measured from the jet inlet axis, with a polar angular range of 50—155 deg. For some of the test points, additional microphones at a sideline distance of 9.17 ft (2.79 m) were also located at large polar angles to minimize interference with the exhaust collector; these microphones were at a different azimuthal angle. Although this was the general microphone layout adopted, other microphone installations were employed for answering specific issues as discussed later. Bruel & Kjaer type 4939 quarter-inch microphones were used for free-field measurements. The microphones were set at normal incidence and without the protective grid, which yields a flat frequency response up to 100 kHz. Narrowband data with a bin spacing of 23.4 Hz were acquired and synthesized to produce one-third-octave spectra, in the range of center band frequencies of 200—80,000 Hz. A detailed description of the instrumentation system and the corrections that need to be applied to the raw spectra may be found in Viswanathan [3]. In some of the earlier tests, both narrowband and one-third-octave filters were used. For comparisons at model scale, the data are corrected to a common distance of 20 ft (6.096 m) from the center of the nozzle exit (coordinate system with origin at the center of the nozzle exit) and standard day conditions: ambient temperature of 77°F (298°K) and relative humidity of 70%. The atmospheric attenuation coefficients are obtained from the method of Shields and Bass [4]; other methods are also evaluated as reported in a later section.

A variety of nozzles, with different diameters D of 1.5 (3.81), 2.45 (6.22), 3.46 (8.8), 4.21 (10.69), 4.71 (11.96), 4.9 (12.44), and 5.34 in. (13.56 cm), and different internal contours were tested. The normalized distance to the microphones r/D, of course, varies with each nozzle used. Aeroacoustic measurements were made for both single jets and dual-stream jets. The test matrix consisted of several series, again depending on the particular issue that was being addressed. For example, for one set of data, the Mach number M of the jet [or nozzle pressure ratio (NPR)] was held constant and the jet stagnation temperature ratio (T_p/T_a for the primary jet and T_s/T_a for the secondary jet in a dual-stream exhaust) was increased progressively, to assess the effect of jet temperature on noise. For the second set, data were acquired at constant jet velocities obtained through the proper choice of NPR and temperature ratio. Nozzles of different diameters were employed to uncover the effects of Reynolds number as well as to address the issue of scaling. Similarly, a comprehensive test matrix was conceived to isolate the contributions of the many noise sources in a dual-stream exhaust system. Realistic geometries and cycle conditions that are representative of modern high-bypass ratio commercial engines were selected. Thus, an extensive database from both single and dual-stream jets has been generated to answer many fundamental questions.

It is of paramount importance to ensure that the acquired data are of high quality, to have confidence in the validity of the conclusions drawn here. Great care and attention were taken during the current tests to ensure that extraneous noise did not cloud the issues. Detailed assessments provided in [1–3] establish unambiguously that the spectra are not contaminated by rig noise. Therefore, this topic is not addressed here.

III. Results and Discussion

Several issues need to be addressed first, before comparisons of model data with engine data can be made. These pertain to the noise measurement system, effects of the flow state, and conditions at the nozzle exit, effects of Reynolds number, atmospheric attenuation corrections, scaling, etc. Some additional related topics are also investigated.

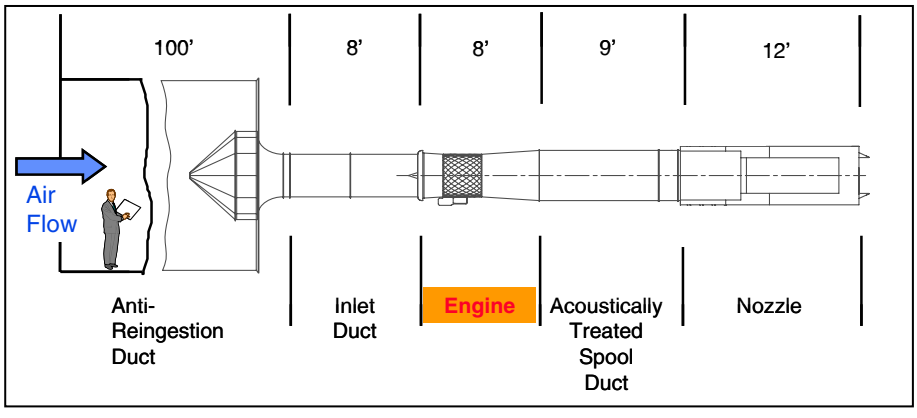

Fig. 4 Schematic of the engine static test setup. Note the size and length of the engine relative to the total length.

A. Impact of the Measurement System

In flight tests and engine static tests, especially for aircraft certification, the highest frequency of interest is usually 10 kHz. However, with smaller models, one needs to obtain accurate spectral measurements up to very high frequencies (it is shown in a later section that it is possible to obtain accurate measurements up to 80 kHz). Spectral measurements at the higher frequencies in model tests are required for scaling of the spectra and allowing direct comparison with engine data. Therefore, the requirements for a model test are more stringent, necessitating a good understanding of the limitations of the measurement system and the adoption of practices that would ensure good measurements at the higher frequencies. It is emphasized again that, for aircraft applications, accurate measurements at all frequencies and at all angles are imperative in a model test. This is particularly so at the higher frequencies, because the scaled spectra fall in the full-scale frequency regime that is most annoying to the human ear and hence penalized heavily in the calculation of the noise metric, such as the effective perceived noise level (EPNL). An inspection of spectra from five different laboratories and reported in [1,2] indicated that the spectral levels at the higher frequencies in all measurements were significantly higher; in most cases, the magnitude of the contamination was more than 5 dB. In some instances, even the spectral trends for simple round jets were incorrect, with the noise levels increasing with frequency rather than the expected roll off to the right of the spectral peak. A comprehensive treatment of the many issues with the instrumentation system that need to be considered for ensuring good quality data is provided in Viswanathan [3]. As shown in [3], the measurement system, in addition to rig internal noise, could contribute to the poor quality of data at the higher frequencies. The salient points are briefly summarized here.

Two different microphone orientations, at either normal incidence or at grazing incidence, are adopted in acoustic tests. For normal incidence, the microphones are usually pointed at the center of the jet at the nozzle exit plane with the implicit assumption that the sources of jet noise can be regarded as a point source concentrated at this location. When the microphones are placed at very large distances, in the true far field of the noise sources, this assumption of a point source is valid and justified. Many anechoic chambers are of limited size, thereby placing constraints on the available distances to the microphones. Provided that the microphones are located in the acoustic and geometric far field, the assumption of a point source is not necessary when the microphones are set at grazing incidence. The great benefit of setting the microphones at grazing incidence is due to the fact that the acoustic rays from a line of distributed sources are always at grazing incidence no matter where the source is located (see Fig. 2 in [3]). That is, no a priori knowledge of the distribution of the jet sources is required with this microphone arrangement. In engine tests, the microphones are usually set at grazing incidence. However, this is not the best arrangement for model tests because of other factors, as described in detail in [3].

The high-frequency sensitivity of condenser microphones varies substantially as the angle of the incident acoustic ray on the microphone diaphragm changes from normal to grazing incidence (see [5]). For aeroacoustic tests at Boeing, the typical choice has been Bruel & Kjaer type 4135 quarter-inch microphones (or the newer type 4939) for normal incidence and type 4136 for grazing incidence, with the as-measured data fully corrected for bias errors in the frequency response of the measurement chain. These corrections are strong functions of frequency: whereas the magnitudes are extremely small ($\sim$0.1 dB) at lower frequencies ($\leq$ 10 kHz), they could add roughly 8–10 dB at the higher frequencies of interest in scale-model tests if the microphones are at grazing incidence (see Fig. 3 in [3]). It is clear then, that though negligible at full-scale frequencies, these corrections could be substantial at model-scale frequencies. Therefore, the instrumentation system should be designed suitably to minimize these corrections. It was demonstrated clearly in [3] that with the application of the appropriate corrections, identical spectral shapes are obtained whether the microphones are set at normal or grazing incidence provided the measurements are made in the true far field.

The second and more important factor pertains to the dynamic range requirements for the measurement system. The dynamic range of the measurement system should be adequate to span the range of the overall sound pressure level and the lowest level of interest at every measurement angle. When narrowband spectrum analyzers are used, the issue of adequate dynamic range becomes more critical; this could be $\sim$80 dB in the peak radiation angles for a high-speed jet as shown in [3]. Contrast this requirement for the model test with that for the high-bypass ratio engine static test. An inspection of Figs. 2 and 3 indicates that the difference between the peak amplitude and the lowest amplitude is only $\sim$30 dB at the aft angles, even at high power. The dynamic range is much less at lower engine power. The contribution from the other sources at the higher frequencies, notably the aft-fan and turbine components, tends to increase the levels at the higher frequencies thereby reducing the dynamic range of the spectra. Therefore, the dynamic range requirements for model-scale tests are more stringent.

There are two important effects due to the distributed nature of the sources of jet noise: one pertains to the measurement aspects of the spectra and the other to the near-field effects. Both of these issues were examined critically in [3]; a brief overview is provided in Sec. III.I here. It was concluded that it is inherently better to orient the microphones at normal incidence and point them at the nozzle exit. Therefore, no confusion should prevail about microphone free-field corrections or the proper design of the instrumentation system.

B. Effect of Atmospheric Absorption

It is well known that the effect of atmospheric absorption is a strong function of frequency, with the coefficients of absorption increasing with increasing frequency. There are also several methods for calculating these coefficients. Two questions need to be addressed:

1) Should the corrections be applied to the narrowband spectra or one-third-octave spectra?

2) Which of the methods is the most suitable for model frequencies and should therefore be used for scaling model data?

First, let us look at the variation of the coefficients for atmospheric absorption at standard day conditions (77°F and 70% relative humidity) with frequency, calculated using the methodologies of Shields and Bass [4], the American National Standards Institute (ANSI) [6], and Society of Automotive Engineers (SAE) ARP866A [7]. Figure 5a shows the variation over a frequency range of 200 Hz–80 kHz; Fig. 5b is a close-up view of the trends for frequencies of interest at engine scale, with an expanded y axis. The SAE method is used for aircraft certification and has been approved by the Federal Aviation Administration (FAA). In the approved procedure, the coefficients are calculated at the one-third-octave center band values for frequencies less than 4 kHz and at the frequencies that correspond to the lower band edge for frequencies above 5 kHz. It is readily apparent from Fig. 5a that the coefficients as given by the SAE method are substantially lower, especially at the higher frequencies. However, it is noted in Fig. 5b that the differences at the lower frequencies (up to 10 kHz) are not large.

We deal with the question of whether one should apply the weather corrections to narrowband data or one-third-octave band data. This issue has practical relevance because the measured spectra must be reduced to some standard conditions. The measured spectrum from an unheated jet at a Mach number of 0.9 at a polar angle of 145 deg is considered to illustrate the two approaches. The spectra were obtained from a nozzle of diameter 1.5 in. (0.0381 m) at a microphone distance of 7.97 m. The raw data are corrected to a distance of 100 D (3.81 m) and to standard day conditions, using the atmospheric absorptions given by Shields and Bass [4]. Narrowband data with a bin spacing of 23.4 Hz were acquired and synthesized to produce one-third-octave spectra, up to a center band frequency of 80,000 Hz. The data have been corrected to 100 D in two ways. First, the atmospheric absorption corrections were applied to the narrowband data and the corrected data were synthesized to one-third-octave spectra. Second, the absorption corrections were directly applied to the synthesized one-third-octave spectra. The

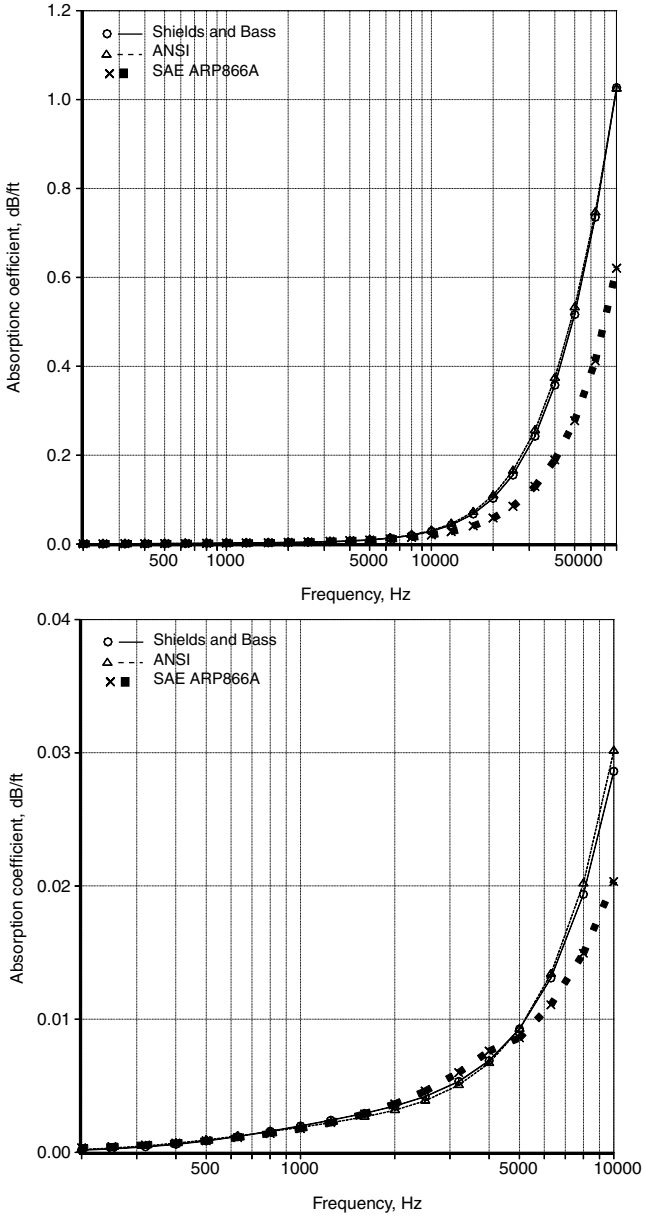

Fig. 5 Variation of the atmospheric absorption coefficient with frequency: a) standard view, b) expanded *y* axis and engine scale frequencies.

results of this exercise are shown in Fig. 6. The symbols represent the as-measured spectrum and the solid line indicates the corrected one-third-octave spectrum. The dotted line was obtained by first applying the corrections to narrowband data followed by the synthesis. It is clear that the two methods produce virtually identical spectra, with the implication that the corrections may be applied to either the narrowband or one-third-octave data. Furthermore, Fig. 6 indicates that even if there is a sharp change in the spectral level within a one-third-octave band (for example, the bandwidth for a center band frequency of 80, 000 Hz spans 70,770–89,160 Hz, with a drop of ∼5 dB in level between the lowest and highest frequencies for this case), there is no difference in the corrected spectra. For a more detailed discussion, see Fig. 6 and associated text in Viswanathan [8].

Next, we investigate the suitability of the different methodologies for practical application to model-scale spectra. A special test has been carried out to answer this question. Four microphones at four different physical distances of 10.59 (3.23), 16.59 (5.06), 22.59 (6.89), and 30.59 ft (9.33 m) from the nozzle exit plane and at a polar angle of 150 deg were installed. These pole-mounted microphones were located at different azimuthal angles to eliminate the

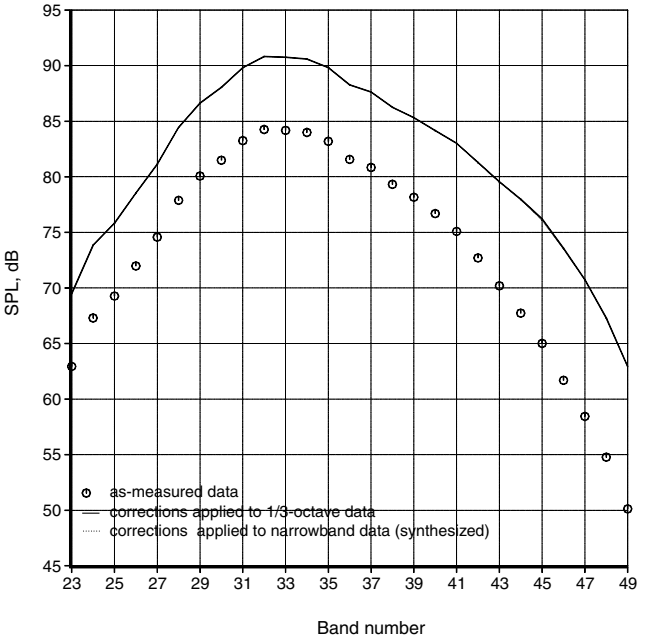

Fig. 6 As-measured and corrected (to 100 D) data. Unheated jet, $M_j = 0.9$, angle = 145 deg.

interference due to the poles, etc. The as-measured spectra from an unheated jet at a Mach number of 0.7 from these four microphones are shown in Fig. 7. First of all, we notice some pronounced wiggles at the lower frequencies in the spectrum measured at 30 ft; these are caused by reflections from the collector lip, due to the proximity of the microphones to the exhaust collector at large distances. See [3] for a detailed analysis of this problem. Apart from this, the spectra are smooth and well behaved. Let us concentrate on the spectra from the two closest mics (top two curves); the difference in the as-measured spectral levels keeps increasing with frequency (from ∼2 dB at 200 Hz to ∼8 dB at 80 kHz), due to the increasing levels of absorption with frequency (as seen in Fig. 5) as the acoustic waves traverse the distance of 6 ft (1.83 m) between the two microphones.

The spectra from the four microphones at different distances have been normalized to a common distance of 20 ft and to standard day conditions, as follows:

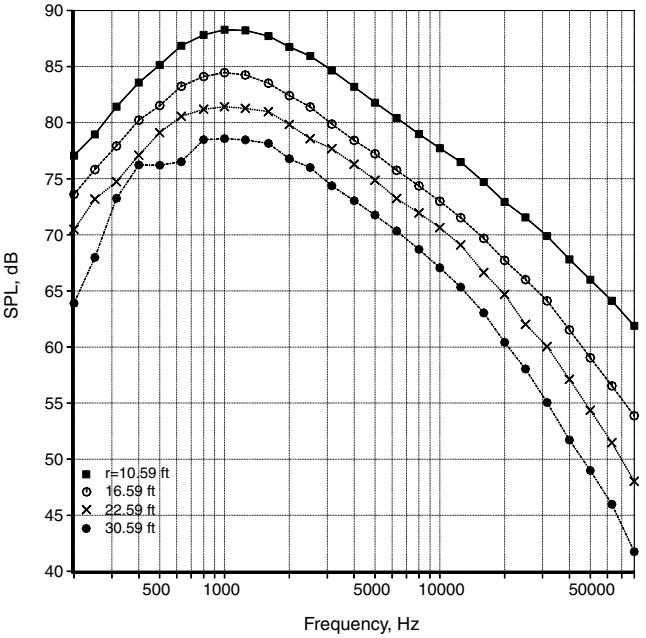

Fig. 7 As-measured data at 150 deg at different microphone distances. Unheated jet, $M_j = 0.7$, $D = 2.45$ in..

$$\mathrm{SPL}_{(20\ \mathrm{ft})} = \mathrm{SPL}_{\mathrm{measured}} - 10\log_{10}\left(\frac{20}{r}\right)^2 + r[\mathrm{AA}_{(\mathrm{test\ day})}] - 20[\mathrm{AA}_{(\mathrm{std\ day})}] \quad (1)$$

where r is the distance (in feet) of the microphone from the origin of the coordinate system, [AA] are the atmospheric absorption coefficients (which are frequency dependent) per foot, and SPL indicates the sound pressure level. The preceding equation provides spectra corrected to standard day conditions; for lossless data, the last term in Eq. (1) is omitted. One can generalize this equation to any observer distance R_o, though it is shown for a reference distance of 20 ft (6.09 m). Implicit in this process is the assumption of linear propagation, with the sound pressure level obeying the $(1/r^2)$ dependence.

The atmospheric absorption coefficients were calculated using the method of Shields and Bass [4]. The normalized spectra, at a Mach number of 0.7 and at two temperature ratios of 1.0 (unheated) and 3.2 are presented in Fig. 8a. There is very good collapse of the spectra over the entire frequency range. It is pointed out that much of the scatter in the data is caused by the measurement at a distance of 30.59 ft (9.33 m), which has been affected by reflections from the lip of the collector (also seen in Fig. 7). Still, the agreement is good at the higher frequencies, because the reflections mostly impact the lower frequencies. If this spectrum is eliminated and the normalized data from the other three microphones are plotted in Fig. 8b, it is clear that there is excellent agreement, especially at the very high frequencies. An examination of Fig. 5a indicates that the absorption values at a frequency of 80 kHz is ~1 dB/ft, as per [4], and ~0.6 dB/ft, as per [7]. The total absorption over a distance of 20 ft (10–30 ft for mic1 and mic4) would be ~20 dB and ~12 dB as per these two methods. The excellent collapse of the data at the higher frequencies seen in Fig. 8 will not be achieved if the absorption values provided by [7] are used, because there would be a mismatch of ~8 dB at 80 kHz. From the sample cases provided here and from the analysis of a larger set of data, it has been conclusively established that the method due to [4] is superior and most suitable for the higher frequencies of interest in model-scale tests. It is recognized that no method is perfect and that there will be small inconsistencies in the values given by any method, especially at extreme weather conditions. However, for engineering applications, the method due to Shields and Bass [4] is deemed satisfactory for the higher frequencies of interest in model-scale tests.

C. Linear and Nonlinear Propagation

The spectra shown in Fig. 7 were normalized with the assumption of a point source for the entire jet centered at the nozzle exit plane. The standard practice of converting the as-measured data to lossless form and then propagating the spectra to a common distance (of 20 ft) while accounting for the atmospheric absorption at standard day conditions has been adopted in the generation of Fig. 8. The assumption of linear propagation, with the sound pressure level obeying the $(1/r^2)$ dependence, was used. This assumption is used widely; as indicated by Fig. 8, it is reasonable and may be justified for many situations. However, this issue has not been examined critically by anyone. Hence, we ask the question: For what jet conditions (velocities) is linear propagation valid?

It is well established that propagation of sound waves with high amplitudes over long distances is subject to nonlinear distortion. Some of the earlier studies on nonlinear propagation are due to Pestorius and Blackstock [9], Blackstock [10], Crighton and Bashforth [11], Gallagher and McLaughlin [12], Howell and Morfey [13], and Gurbatov et al. [14], among others. These studies established that the nonlinear distortion resulted in the steepening of the waveforms, a decrease in the zero crossings of the wave due to the coalescence of shock waves, and the transfer of energy from the spectral peak to both the low- and high-frequency portions of the spectra. Most of the experimental measurements used to identify nonlinear propagation have been obtained in outdoor test facilities or from aircraft flight tests for jet noise, for example [13], or in long pipes for plane wave propagation (for example see [9]). The

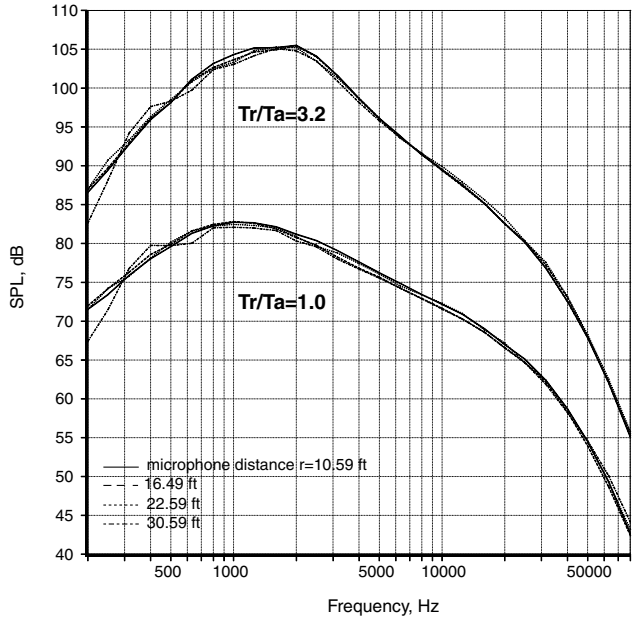

Fig. 8 Data normalized to 20 ft and standard day conditions from measurements at different microphone distances. Angle = 150 deg, $M_j = 0.7$, $D = 2.45$ in..

difficulties associated with making good measurements in outdoor test stands are well known; a host of corrections need to be applied to the raw data. These corrections are subject to uncertainties in the varying weather conditions between the source and the measurement points, varying impedance of the terrain, temperature inversions near the ground, possible interference of the direct and reflected signals in an unknown fashion, etc. The spectra from these tests are seldom clean and hence not perfectly suited for the assessment of methods for nonlinear propagation. Thus, there is a clear need for benchmark data as well as better methods for the prediction of nonlinear propagation. An important objective of this set of measurements is the creation of high-quality pressure-time signals obtained in a controlled environment in a large anechoic chamber that can be used for the development/refinement of algorithms for nonlinear propagation.

We now present data that indicate that nonlinear propagation occurs even in laboratory tests, where the propagation distances are

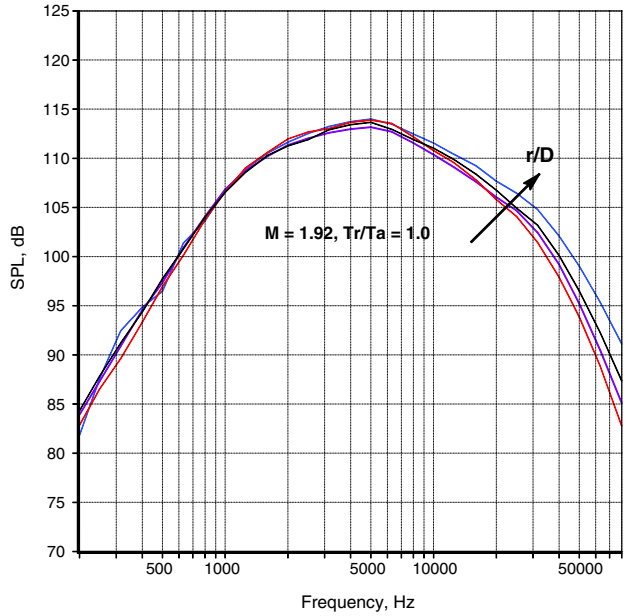

Fig. 9 Data normalized to 20 ft and standard day conditions from measurements at different microphone distances. Angle = 150 deg, $D = 1.27$ in., $r/D = 100, 157, 213, 289$.

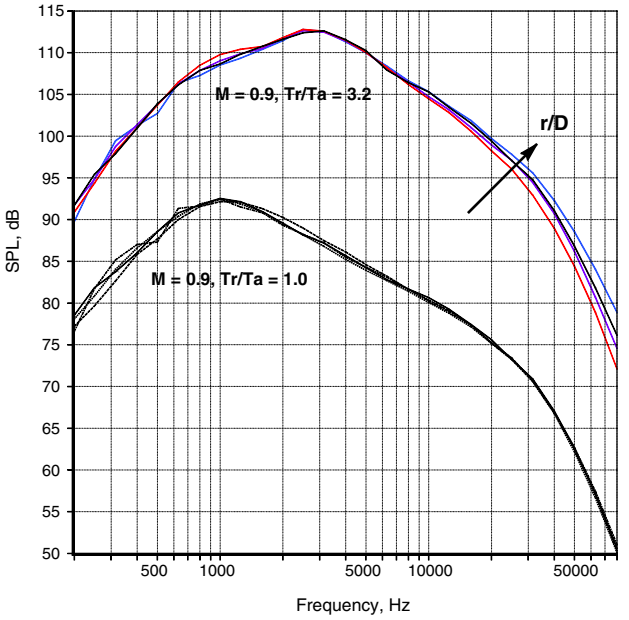

Fig. 10 Data normalized to 20 ft and standard day conditions from measurements at different microphone distances. Angle = 150 deg; Upper curves: $r = 10.59, 16.59, 22.59, 30.59$ ft.

several orders of magnitude smaller than those observed in outdoor flight tests. Figure 9 shows normalized data from the four microphones for a supersonic jet at a Mach number of 1.92. Clearly, the levels at the higher frequencies keep increasing with propagation distance and the excellent collapse observed in Fig. 8 is not seen for the supersonic jet. Additional analysis of this set of data is provided in [15]. This phenomenon has been noted in other studies as well for supersonic jets.

We show a comparable plot for an unheated and a highly heated ($T_r/T_a = 3.2$) jet at a Mach number of 0.9 in Fig. 10. There is very good collapse of the spectra for the unheated jet, as seen in Fig. 8. However, for the highly heated jet, nonlinear propagation effects, similar to those seen for the supersonic jet in Fig. 9, begin to appear. This is surprising and unexpected, because neither the jet velocity nor the amplitude level is particularly high for this case. Further analysis reveals that the convective Mach number M_c, defined as the ratio of the convective velocity to the ambient speed of sound, just becomes supersonic for the $M = 0.9$ jet at a temperature ratio of 3.2. It has been established from experimental measurements that the average convective velocity is $\approx$70% of the mean jet velocity; this value has been assumed in the calculation of M_c. The question that needs to be answered is whether the onset of nonlinear propagation occurs suddenly when the convective Mach number becomes supersonic or if there is a gradual progression to nonlinear propagation as the convective Mach number is increased systematically. We now present normalized spectra from two microphones at radial distances of 16 ft (4.88 m, $r/D = 78$) and 26 ft (7.93 m, $r/D = 128$) and at a polar angle of 145 deg. As before, the spectra are converted to standard day conditions and corrected to a common distance of 20 ft (6.09 m). The jet temperature ratio is 3.2 and the Mach number is progressively increased from 0.6 to 1.0 in steps of 0.1. Figure 11 shows spectral comparisons at the five Mach numbers. The convective Mach numbers and the overall sound pressure levels (OASPL) measured at the nearer microphone ($r/D = 78$) are shown in Table 1. Also shown is the Doppler correction factor $(1 - M_c \cos\theta)$ for three different angles measured from the jet exhaust. These values are discussed in Sec. III.E and hence should be ignored for the time being.

Figure 11 indicates that there is good collapse of the data for the lower Mach numbers of 0.6, 0.7, and 0.8; the convective Mach numbers are also subsonic for these cases. When the jet and convective Mach numbers are increased, we notice the onset of nonlinear propagation effects at the higher frequencies, with only minor changes at the lower frequencies. Note that the convective Mach numbers are supersonic for the higher two Mach numbers. It has been generally believed that nonlinear phenomena are observed only at very high sound pressure levels (typically $\sim$145 dB). However, the OASPL for the $M = 0.9$ jet is only 123.8 dB at a distance of $r/D = 78$. If we assume inverse-square dependence for OASPL, the levels would still be only 129.8 dB for $r/D = 39$, which is just beyond the edge of the near field (see Sec. III.I). This level is considerably less than the levels quoted in the literature. We propose here that the convective Mach number, rather than the amplitude of sound, is a good indicator of nonlinear propagation effects for jet noise and hence be examined to discern nonlinear processes. This phenomenon has been completely missed by everyone in over 50 years of jet noise research! Evidence presented for the first time in Fig. 11 and other data (not shown) clearly indicate that the assumption of linear propagation in data processing is valid only when the convective Mach number is subsonic. There is no methodology currently available for calculating the nonlinear propagation effects. Further study is clearly warranted and is currently underway, with detailed flowfield measurements as well as the noise levels in the acoustic near and far fields from heated and unheated jets over a wide range of convective Mach numbers, to glean the underlying physics. A parallel computational study and

Table 1 Tabulation of jet Mach number, convective Mach number, and OASPL, $T_r/T_a = 3.2$

M	M_c	OASPL, dB	$[1 - M_c \cos(55)]$	$[1 - M_c \cos(50)]$	$[1 - M_c \cos(35)]$
0.6	0.735	110.0	0.578	0.528	0.398
0.7	0.840	115.2	0.518	0.460	0.312
0.8	0.945	119.4	0.458	0.393	0.226
0.9	1.057	123.8	0.394	0.321	0.134
1.0	1.148	126.6	0.342	0.262	0.060

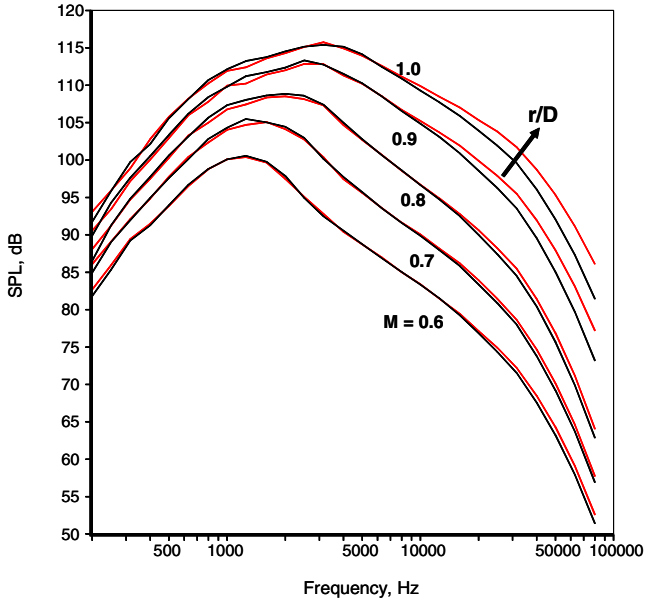

Fig. 11 Data normalized to 20 ft and standard day conditions from measurements at two different microphone distances. Angle = 145 deg, $T_r/T_a = 3.2, r/D = 78, 128$.

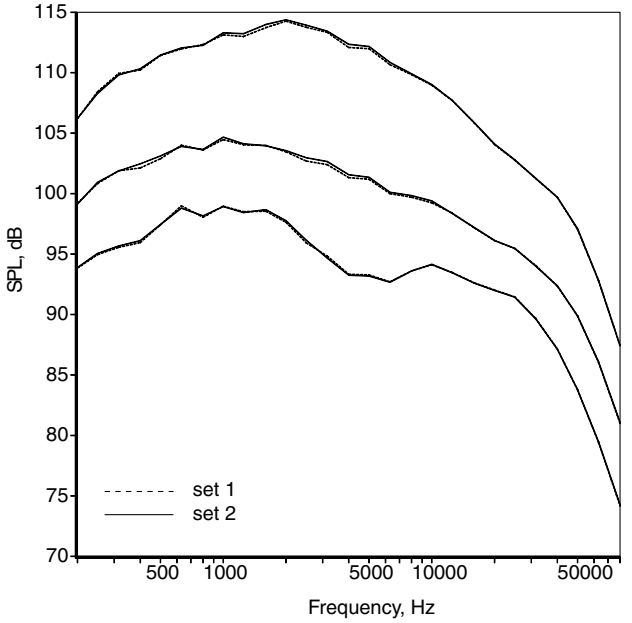

Fig. 12 Comparison of spectra at 130 deg at three power settings.

these experiments are being carried out collaboratively with the researchers at The Pennsylvania State University, and the results will be reported in the future. Note that only a slight reduction in spectral level at the peak would be adequate to transfer energy to the higher frequencies (and to the lower frequencies) because the peak one-third-octave level is ~25 dB above the levels at the two extreme frequency regimes.

D. Repeatability of Data

The scatter in experimental data from various laboratories is a cause for concern because the absolute noise levels for a given jet velocity cannot be established with certainty. This problem becomes more critical when concepts for noise suppression are evaluated. A comprehensive study of issues related to rig noise and the instrumentation system were provided in [1,3], respectively. Here, we concern ourselves with the following question: How repeatable are jet noise measurements? Sample data from a variety of nozzles are provided to illustrate data repeatability.

First, we present data taken a few weeks apart, with a mixer/ejector nozzle geometry in Fig. 12. There is excellent agreement between the repeat runs at the three power settings. The data were normalized to standard day conditions. Viswanathan [3] provides additional details about this test; from an analysis of a larger data set, it was noted in this reference that the deviations were within ±0.25 dB at all angles and all frequencies (see Fig. 10 in [3]). Next, we show data from a compound flow nozzle with an internal lobed mixer, with both streams heated and at a cycle condition that corresponds to takeoff power, in Fig. 13. The spectra, shown over a wide polar angular range, were acquired about one year apart; one set was taken in summer and the other one in late fall, with the ambient weather conditions being different. Further, repeated assembly and teardown of the nozzle hardware could result in slight variations in geometric fit, nozzle orientation, etc. Again, there is excellent agreement between the two sets of normalized data. The same jet rig was used as in the preceding tests.

Finally, we verify if it is possible to acquire the same levels of noise from the same nozzle hardware, but with two different jet rigs. These measurements were carried out ~20 years apart; of course, the electronics and the measurement systems evolved considerably during this time period. In the old measurements, a blowdown rig with extremely low rig noise was used; in the latter test, a compact rig was used. The compact rig was also incorporated with a six-component force balance, with the attendant complexities and

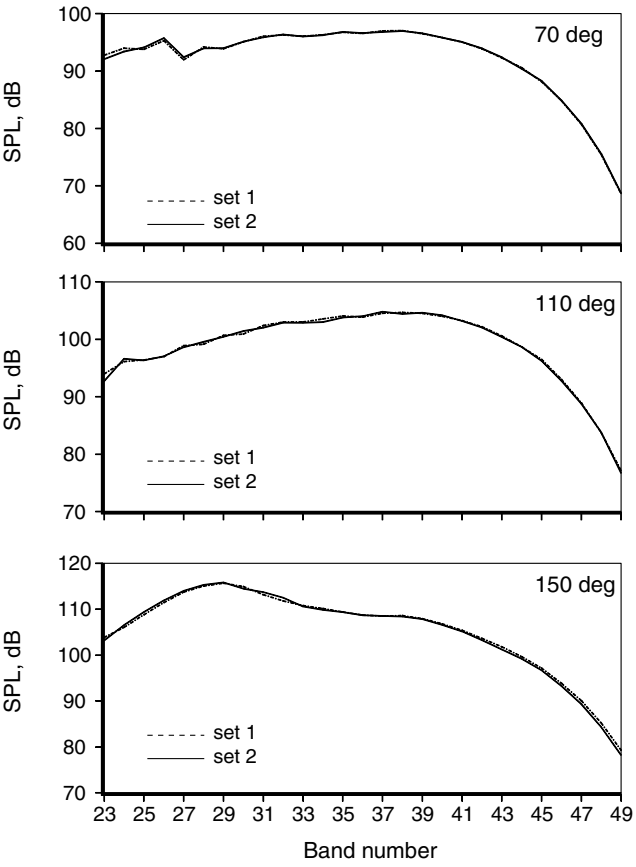

Fig. 13 Comparison of spectra at various polar angles. Compound flow nozzle, high power.

additional challenges for accurate noise measurements. Viswanathan [1] provides detailed descriptions of these jet rigs and issues with data quality. Two sample results from dual-stream nozzles are provided here in Figs. 14 and 15, at low and high power. The jet conditions are as follows: $\mathrm{NPR}_p = 1.24$, $T_p = 1394$ deg R, $\mathrm{NPR}_s = 1.34$, $T_s = 600$ deg R for Fig. 14 and $\mathrm{NPR}_p = 1.88$, $T_p = 1455$ deg R, $\mathrm{NPR}_s = 1.8$, $T_s = 540$ deg R for Fig. 15. (Subscripts p and s denote primary stream and secondary stream, respectively.) There is excellent agreement between the two sets of spectra, especially in the

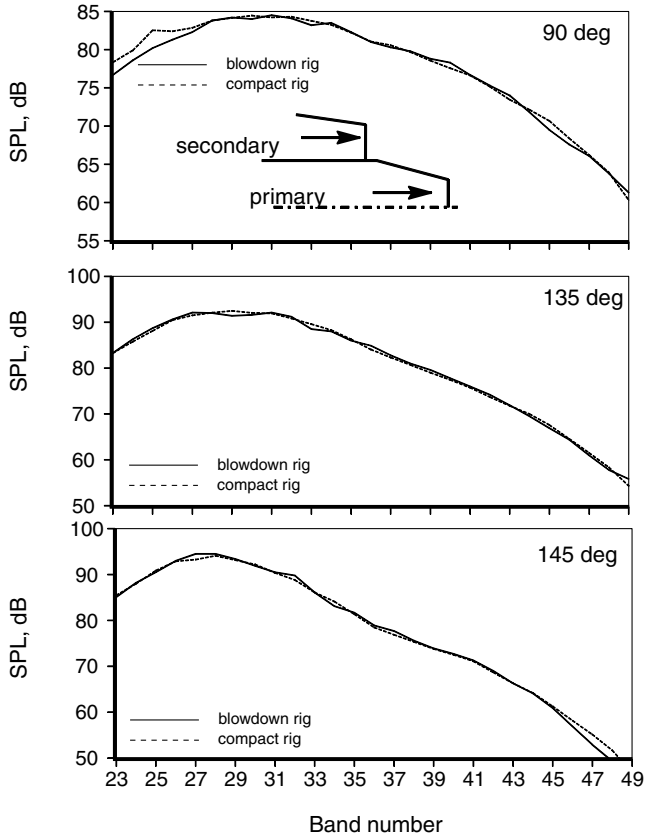

Fig. 14 Comparison of spectra from compact rig with blowdown rig. Coaxial nozzle, $A_s/A_p = 3.0$.

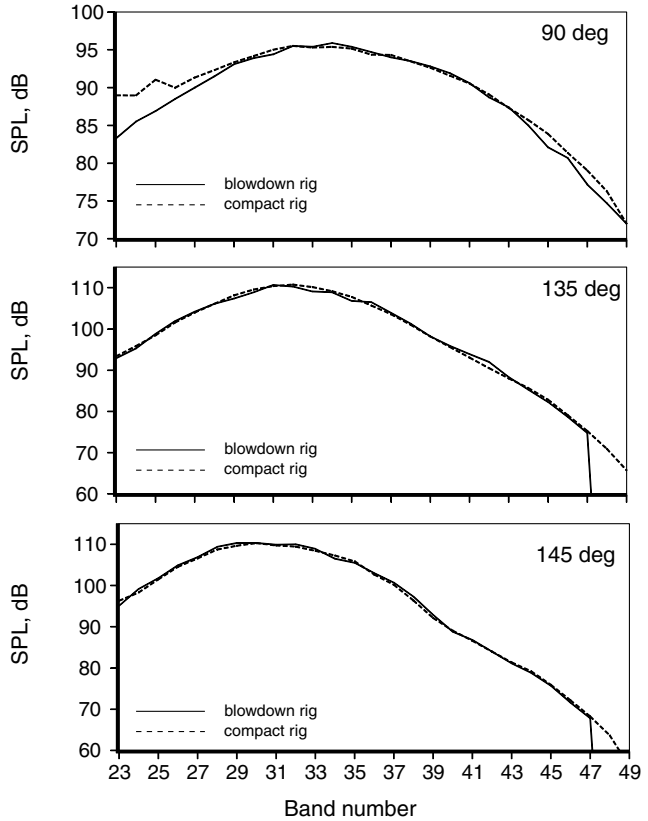

Fig. 15 Comparison of spectra from compact rig with blowdown rig Coaxial nozzle, $A_s/A_p = 3.0$.

peak radiation angles. There are some tones at the low frequencies, more prominent at the lower radiation angles; the cause of these tones were investigated and discussed in [1].

The preceding comparisons, from a variety of nozzle configurations, indicate that it is possible to acquire consistent and repeatable jet noise data, with meticulous attention to detail and the adoption of good experimental practices. It should be appreciated that even the best manufactured nozzles are not perfectly symmetric and therefore the noise fields are not entirely axisymmetric. Given the slight variability in the microphone characteristics, mic-to-mic variation in their responses and mounting schemes, and slight errors in the calculation of atmospheric absorption coefficients, it is gratifying that there is such excellent spectral agreement in Figs. 12–15 here, and in [1,3]. One cannot overstate the importance of proper planning, design, and execution of aeroacoustic tests to attain such good results. It should be further noted that the model-scale tests are carried out in anechoic chambers, with controlled environments. The scatter in data would be higher in outdoor test stands where the ambient noise levels could be high and the variability in weather conditions such as temperature gradients and changing wind speed and direction necessarily introduce some uncertainty.

It is important not to confuse repeatability with accuracy. In many of the examples shown in [1], in which the magnitude of the contamination was ~5 dB or more, the spectra were highly repeatable though completely off. One should employ other methods to assess data quality. However, if the spectra keep changing with repeat measurements, the situation is entirely hopeless because one can never know the true levels. This is especially so when evaluating noise reduction concepts.

E. Scaling of Jet Noise Spectra

The issue of scaling of the spectra at model scale is discussed in detail, because the normalized spectra are used to clarify certain issues; comparisons with engine measurements are deferred until a later section. Sample comparisons are provided to identify the different normalization factors as well as to assure the reader about data quality. Equation (1) simply corrects the data to a desired observer distance. For what is to follow, a more thorough analysis is needed. We start with the gas dynamic equations for a flow through a nozzle. For a nozzle operating at a nozzle pressure ratio of (p_t/p_a) and reservoir total temperature ratio of (T_r/T_a), the expressions for the ideal mass flow rate $\dot{m}$, ideal jet velocity V_j, and ideal thrust F, may easily be derived in terms of the nozzle reservoir conditions. These quantities may be expressed as follows:

$$\dot{m} = p_t A M \sqrt{\frac{\gamma}{RT_r}}\left[1 + \frac{\gamma - 1}{2} M^2\right]^{-[(\gamma+1)/2(\gamma-1)]} \tag{2}$$

$$V_j = \sqrt{2RT_r\left(\frac{\gamma}{\gamma - 1}\right)\left[1 - \left\{\frac{p_t}{p_a}\right\}^{-[(\gamma-1)/\gamma]}\right]} \tag{3}$$

$$F = \dot{m} V_j \tag{4}$$

In the preceding expressions, p_t is the plenum total pressure, A is the throat area, T_r is the plenum total temperature, R is the gas constant, and γ is the ratio of specific heats. To facilitate comparisons on the same normalized basis when nozzles of different diameters are tested at the same plenum conditions, the thrust must be maintained constant. This is easily accomplished by calculating thrust per unit flow area, using the preceding equations:

$$\frac{F}{A} = p_t M \gamma \left[1 + \frac{\gamma - 1}{2} M^2\right]^{-[(\gamma+1)/2(\gamma-1)]} \times \sqrt{\left(\frac{2}{\gamma - 1}\right)\left[1 - \left\{\frac{p_t}{p_a}\right\}^{-[(\gamma-1)/\gamma]}\right]} \tag{5}$$

Note that the terms on the right-hand side contain only the plenum conditions and the effect of the nozzle area is removed. Similarly, when comparing noise, the effect of the different nozzle exit areas can be scaled out by computing the noise per unit area. There could be minor differences in the nozzle discharge coefficients C_d depending on the nozzle design and the Reynolds number of the flow, thereby yielding slightly different actual mass flows. Typically, well-designed nozzles have discharge coefficients of ~0.98 to ~0.99, especially at realistic Reynolds numbers. Similarly, there could be minor variations in the thrust coefficientC_f as well (see Fig. 8 in [16] for example). In acoustic tests at engine and model scales, the engine cycle conditions (NPR and stagnation temperature) are matched exactly. Thus, the thermodynamic states are identical except for the difference in the physical size. It should be clear that scaling noise per unit flow area is equivalent to maintaining constant thrust at different scales. The effect of the minor variations due to different discharge coefficients may be estimated as $[10 \cdot \log_{10}(C_{d1}/C_{d2})]$. The difference in noise because of this effect, as well as due to changes in the thrust coefficient, is ~0.1 dB, which is negligible and is therefore ignored here. The sound pressure level is expressed in logarithmic scale, therefore, the subtraction of the term $[10 \cdot \log_{10}(A)]$ normalizes the sound pressure level for constant thrust. There are subtle intricacies when scaling narrowband spectra; it is important to scale the amplitude of the SPL per unit Strouhal number so as to maintain the same acoustic energy, a result established many years ago. This requirement leads to the subtraction of an additional term $[10 \cdot \log_{10}(D/V_j)]$; see [17] in which the issues with scaling one-third and narrowband data are revisited.

Normalized spectra from unheated jets at three Mach numbers of 0.8, 0.9, and 1.0 and from three nozzles of diameters 1.5, 2.45, and 3.46 in. are presented in Fig. 16. The spectra have been normalized to a common distance of 20 ft (6.09 m) using Eq. (1). First, we demonstrate that the scaling of spectra can be carried out with both narrowband and one-third-octave spectra. For narrowband data, the spectra are normalized as follows: the effect of nozzle diameter on spectral levels is scaled out and the parameter $[\mathrm{SPL} - 10 \cdot \log_{10}(A) - 10 \cdot \log_{10}(D/V_j)]$ (A is the nozzle exit area) is plotted against the Strouhal number (fD/V_j, where f is the frequency in Hertz) in Fig. 16a, at two Mach numbers of 0.8 and 1.0. The spectra at a polar angle of 145 deg, corrected to lossless conditions using the method of [4] are shown. As seen, there is excellent collapse of the two sets of spectra over the entire frequency range. The one-third-octave spectra are normalized as follows: the effect of nozzle diameter on spectral levels is scaled out and the parameter $[\mathrm{SPL} - 10 \cdot \log_{10}(A)]$ is plotted against the Strouhal number. The spectra at the same polar angle of 145 deg, corrected to lossless conditions using the method of [4] at three Mach numbers of 0.8, 0.9, and 1.0, are presented in Fig. 16b. The curves have been spaced apart to enhance visual observation and hence do not represent the noise increase due to the higher jet velocities. As seen, there is excellent agreement throughout the frequency range when the noise per unit flow area (or constant thrust) is examined.

Some researchers adopt another method of scaling spectra, wherein the spectral levels are corrected to a distance of (100 D). This approach, if done correctly, seemingly leads to satisfactory scaling for the following reason. Because the acoustic intensity generally varies as $(1/r^2)$, we can use Eq. (1) and write

$$\mathrm{SPL}_{(100\,\mathrm{D})} = \mathrm{SPL}_{\mathrm{measured}} - 10\log_{10}\left(\frac{100\,\mathrm{D}}{r}\right)^2 + r[\mathrm{AA}_{(\mathrm{test\ day})}] - 100\,\mathrm{D}[\mathrm{AA}_{(\mathrm{std\ day})}] \tag{6}$$

The second term on the right-hand side has the term $[-10 \cdot \log_{10}(D)^2]$. It was shown before that for comparing noise at constant thrust, the parameter $[\mathrm{SPL} - 10 \cdot \log_{10}(\pi D^2/4)]$ must be examined at a fixed distance. Note that the only difference with the second approach is the factor $(\pi/4)$ $[10 \cdot \log_{10}(\pi/4) = -1.05$ dB]. That is, the effects of the different nozzle areas and different thrust levels are implicitly accounted for by the spherical divergence function. However, whereas the scaling formula described here is based on normalizing the SPL for constant thrust and to a common distance, there is no physical basis for correcting the data to (100 D).

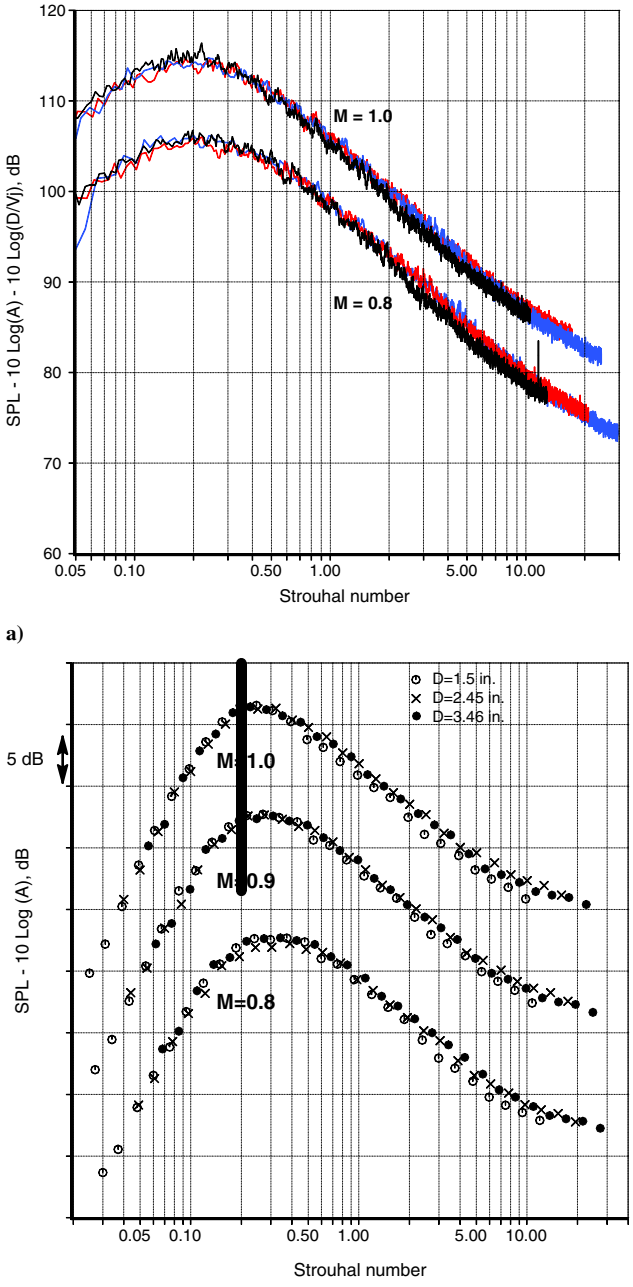

Fig. 16 Comparison of normalized spectra from unheated jets. Angle = 145 deg, D = 1.5, 2.45, 3.46 in., a) narrowband spectra, b) one-third-octave spectra.

It is worthwhile to discuss some additional corrections or normalization terms that would be necessary to account for the day-to-day variations in the ambient conditions, such as pressures and temperatures. Several expressions have been developed since the mid-1970s. These correction terms are typically expressed in terms of the mismatch between the ambient pressures and temperatures with standard day pressures and temperatures. More elaborate forms of these terms have also been developed by several researchers. The magnitudes of these corrections usually tend to be small and have not been applied here. Figure 13 indicates that even without these small adjustments, good agreement is achieved. The changes in the ambient conditions could also change the jet velocity and the ambient speed of sound a slightly. This effect on noise, usually small, can be scaled out by using the measured V_j and the ambient speed of sound for a given test day, as shown next.

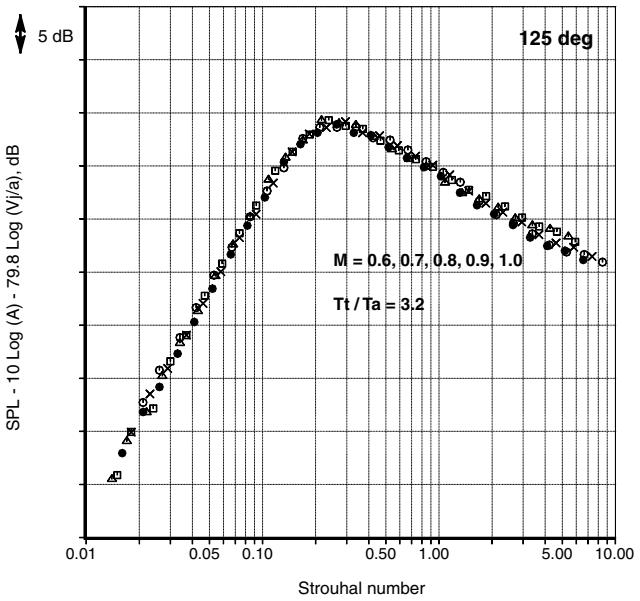

Fig. 17 Comparison of normalized spectra from heated jets. angle = 125 deg, $D = 1.5$ in..

The V^8 dependence of overall power has been well known for over 50 years. Viswanathan [2] showed, however, that the temperature ratio plays an important role in setting the velocity exponent, both for the overall power level (OAPWL) and the overall sound pressure level (OASPL) at any angle. A detailed discussion is provided in Sec. 4.4 in [2] and in [18]. It is important to recognize that the velocity exponent could be different from a value of eight, depending on the jet temperature ratio and radiation angle. In Fig. 17, the effect of the jet velocity is removed and the parameter $[\mathrm{SPL} - 10 \cdot \log_{10}(A) - 80 \cdot \log_{10}(V_j/a)]$ is plotted against the Strouhal number. These spectra were obtained from highly heated jets with a temperature ratio of 3.2 and were at Mach numbers of 0.6, 0.7, 0.8, 0.9, and 1.0. Again, there is excellent collapse of the normalized spectra throughout the frequency range. The angles of 145 and 125 deg were chosen for specific reasons. As noted, the velocity exponent varies with the radiation angle and the jet temperature. Typically, this value increases with increasing inlet angle and decreases as the jet temperature is progressively increased. It just so happens that the value of roughly eight is reached at 125 deg, whereas it is 5.53 at 90 deg. In Fig. 18a, we collapse the data shown in Fig. 16b through the elimination of the velocity effect. Specifically, the term $[\mathrm{SPL} - 10 \cdot \log_{10}(A) - 96.4 \cdot \log_{10}(V_j/a)]$ is plotted. That is, a velocity exponent of 9.64 is seen to collapse the data; clearly, the sound pressure level in this direction does not scale with a value of eight. This point is discussed in greater detail by Viswanathan [18], where the velocity exponent is calculated for a wide range of angles and for several temperature ratios.

So far, attention has been paid to the scaling of the SPL amplitudes. Now, the scaling of the frequency is examined; note that the Strouhal number has been used in Figs. 16–18. Lush [19], among others, initially proposed that the Doppler corrected Strouhal number $[[f(1 - M_c \cos\theta)D/V_j]]$ is the proper choice for scaling the frequency. This suggestion was followed widely by the theoreticians in the 1970s and early 1980s in analyzing jet noise data, and developing scaling laws and theoretical models. The term $(1 - M_c \cos\theta)$ also appears prominently in the directivity factor, as proposed by Lighthill [20] and subsequently modified and extended by others. The suitability of the Doppler correction for the frequency is investigated with the current database. Table 2 shows the jet Mach numbers, the corresponding convective Mach numbers, and the Doppler factor for three angles, for heated jets with a temperature ratio of 2.2. Comparable values were provided in Table 1 for jets with $T_r/T_a = 3.2$.

The lower temperature case has been chosen because the convective Mach number is subsonic for all jet Mach numbers, and

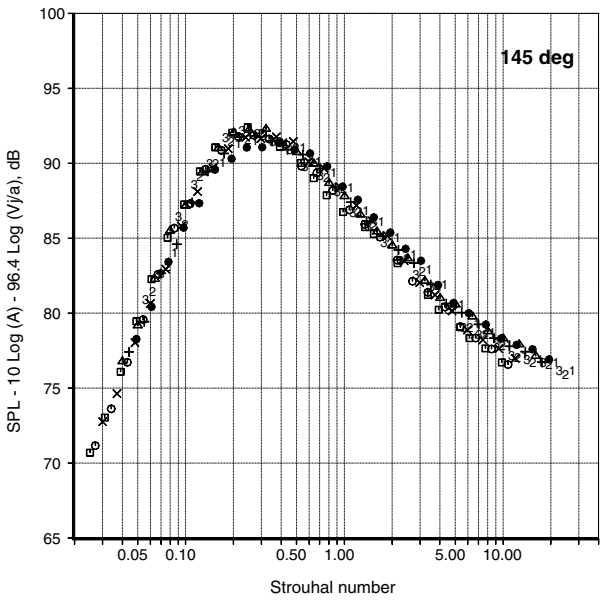

a)

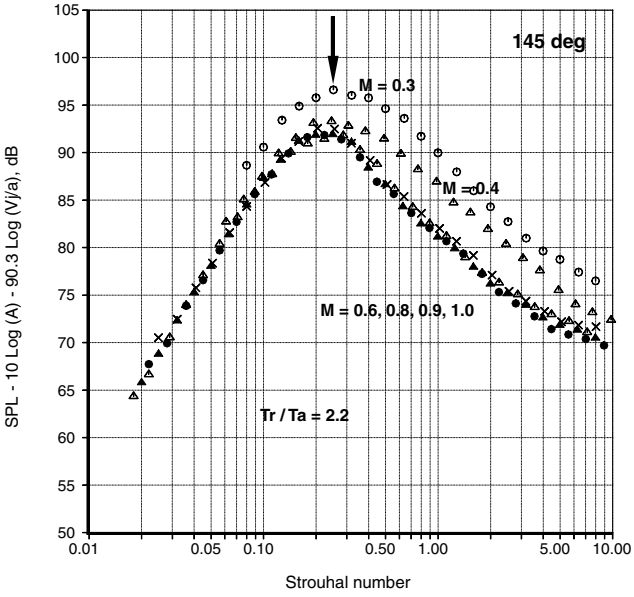

b)

Fig. 18 Comparison of normalized spectra from a) unheated jets, $M = 0.8$, 0.9, and 1.0, $D = 1.5$, 2.45, and 3.46 in., and b) heated jets, $T_r/T_a = 2.2$.

complications with nonlinear propagation are avoided. Figure 18b shows normalized spectra at an inlet angle of 145 deg ($\theta = 35$ deg) plotted against the Strouhal number without the Doppler correction. The Mach numbers span a wide range of 0.3–1.0. First of all, there is excellent collapse of the spectra for the higher Mach numbers over

Table 2 Tabulation of jet Mach number, M_c, and Doppler factor, $Tr/T_a = 2.2$

M	M_c	$[1 - M_c \cos(55)]$	$[1 - M_c \cos(50)]$	$[1 - M_c \cos(35)]$
0.3	0.301	0.827	0.807	0.753
0.4	0.413	0.763	0.735	0.662
0.5	0.511	0.707	0.672	0.581
0.6	0.609	0.651	0.609	0.501
0.7	0.700	0.598	0.550	0.427
0.8	0.784	0.550	0.496	0.358
0.9	0.875	0.498	0.438	0.283
1.0	0.952	0.454	0.388	0.220

the entire frequency range; the lower Mach number spectra are obviously contaminated by rig noise, with the levels being higher by ~4 dB for the $M = 0.4$ jet over a wide range of higher frequencies. The level of contamination is much higher for the $M = 0.3$ jet. (This issue of noise contamination at low Mach numbers has been dealt with in great detail in [1,2].) Let us examine the spectral shape and the alignment of the spectral peaks, while fully recognizing the effect of the rig noise leading to elevated levels at the lowest two Mach numbers. It is clear that the spectral peaks are perfectly aligned at a Strouhal number of ~0.25, as denoted by the arrow in Fig. 18b. The ratio between the Doppler factors in Table 2 for the lowest Mach number of 0.3 (0.753) and the highest Mach number of 1.0 (0.22) is 3.42. If we use the Doppler correction for the frequency on the x axis, the spectral peaks for these two Mach numbers will be spread apart by a factor of 3.42! Furthermore, each of the spectra at the other Mach numbers will be subjected to varying Doppler correction factors and the perfect collapse and the alignment of the peaks will be completely destroyed. Similarly, the perfect collapse of the spectra at a lower angle of 125 deg in Fig. 17 will be lost with the application of the Doppler correction factor for frequency. Excellent collapse of the entire spectra with the Strouhal number, at different temperature ratios, has been provided at various aft angles of 110, 120, 125, 130, 135, and 145 deg here and in Viswanathan [18,21]. At further aft angles of 155 and 160 deg, Viswanathan [21] demonstrated perfect collapse of the spectra with the Helmholtz number (fD/a) for unheated jets, and emphasized that the right velocity exponent (=9.8) as well as the right characteristic velocity scale (a, the ambient speed of sound) must be used. Again, the Doppler correction was not needed for these two angles as well. As such, there seems to be no justification for the use of the $(1 - M_c \cos\theta)$ term for normalizing frequency. Though there could be some theoretical basis for its inclusion, as propounded by Lush [19] and others, there is no experimental evidence to support this contention. The strong influence of the jet temperature ratio on the spectral shape at aft angles was identified in [18] (see Sec. V). The data presented here and in [18,21] cast major doubts on the validity of the concept of convective amplification and the use of the Doppler factors.

Though not explicitly mentioned here, it should be obvious that the preceding scaling methodology has an important application, that of checking data quality. The normalization process, as shown in Fig. 18b for example, helps to identify the magnitude of the contamination by rig noise and the affected frequencies at the lower two Mach numbers in a quantitative manner. Whereas pure jet noise follows the scaling law, the rig noise does not and hence can be detected easily. Contrast this trend with the normalized spectra shown in Fig. 17, in which there is excellent collapse, denoting the absence of any contamination. This application is described in greater detail in [21].

Finally, we show that the preceding scaling is valid even for shock-containing plumes. Figure 19 shows the normalized spectra from unheated jets at two Mach numbers of 1.36 and 1.56 from the same three conical nozzles. The fully expanded jet diameter is used for scaling frequency as well as the nozzle area. There are strong screech tones from all the nozzles, with the amplitude from the smallest nozzle being the highest. At $M = 1.36$ (lower set of curves), there is excellent agreement in levels for the turbulent mixing noise component, which can be identified to the left of the prominent screech tone. It is also well established from the experiments at NASA Langley Research Center, see Seiner [22] and Tam et al. [23], that strong screech tones tend to amplify the turbulent mixing noise. At the higher Mach number, where the screech tones are even stronger for the smallest nozzle, the spectra from only the two large nozzles are shown. We see that there is excellent collapse over the entire frequency range again for the narrowband data. It is clear then that the scaling of the spectra can be performed with narrowband or one-third-octave spectra, provided it is done properly. Given this equivalency, it is a matter of choice as to which is adopted. The use of one-third-octave spectra has an important advantage: precise assessments of the atmospheric absorption methods (Figs. 8b and 10), data repeatability (Figs. 12 and 13), and spectral collapse (Fig. 17) are possible. Good narrowband spectra have wiggles with amplitudes of ~2 to ~3 dB (Fig. 16a), which prevent exact comparisons. These wiggles in the narrowband data also tend to be somewhat distracting and hence the author prefers to work with one-third-octave data, even though only narrowband data are acquired in the laboratory tests.

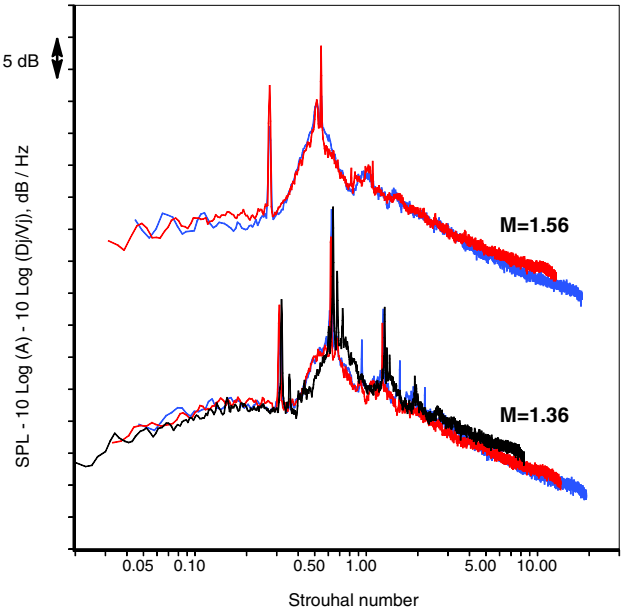

Fig. 19 Comparison of normalized spectra from unheated jets; angle = 90 deg, $D = 1.5, 2.45, 3.46$ in.

F. Effect of Reynolds number

There is a vast disparity in the Reynolds number between model nozzles and jet engines. One needs to consider if there are any effects on noise associated with the lower Reynolds number in model tests and if these effects would play a role in the comparison of scaled model spectra with engine data. In nearly 50 years of noise research, it was never suspected that the Reynolds number could have an effect on the jet noise spectra. This is in spite of the well-established fact that at lower Reynolds number, the nozzle discharge coefficient has lower values. Only recently, Viswanathan [2] carried out a careful study to specifically quantify the effects of Reynolds number on noise. The salient results from this study are summarized next.

Data were presented from three nozzles of different diameters (same as those shown in Fig. 16) over a wide range of Mach numbers and temperature ratios. First, it was shown that the spectral shape at the lower polar angles does change with increasing temperature, with an extra hump near the spectral peak, especially at lower Mach numbers. This trend had been noted in the experimental measurements in the 1970s and the extra hump had been attributed to the contributions from an additional dipole source for hot jets. To aid the discussion, two of the figures from [2] are reproduced here as Figs. 20 and 21. Figure 20 summarizes the findings in Sec. 4.2 of [2] and brings out the effect of Reynolds number explicitly. The spectra at 90 deg from a jet of Mach number 0.7 and temperature ratio 3.2 from three nozzles of diameters 1.5, 2.45, and 3.46 in. and comparisons with the fine-scale similarity spectrum (FSS) of [23] are shown. The extra hump is obvious in the spectra obtained with the smallest nozzle ($D = 1.5$ in.). The magnitude of the discrepancy between the data and the similarity spectrum near the spectral peak decreases for the nozzle with $D = 2.45$ in. and almost completely disappears for the largest nozzle. The only parameter different in the three cases is the Reynolds number, with values of 204,000, 333,200, and 470,600 for the three nozzles, respectively. Figure 21 provides a quantitative measure of the change in spectral shape due to Reynolds number, with a comparison of the normalized spectra for the various Mach numbers of 0.6, 0.7, 0.8, 0.9, and 1.0 and at a temperature ratio of 3.2. The spectra obtained with the smaller nozzle ($D = 1.5$ in.) and denoted by the open symbols collapse to a single curve. The

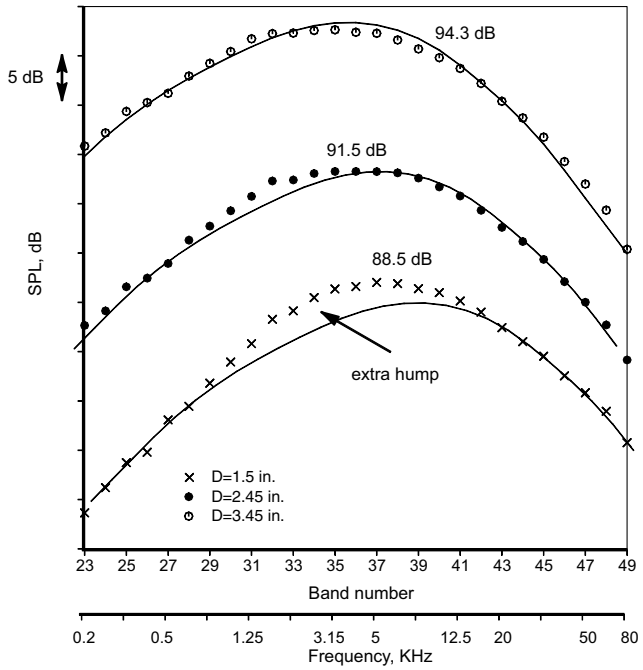

Fig. 20 Comparison of measured spectra with fine-scale similarity spectrum; $M = 0.7$, $T_r/T_a = 3.2$, angle = 90 deg.

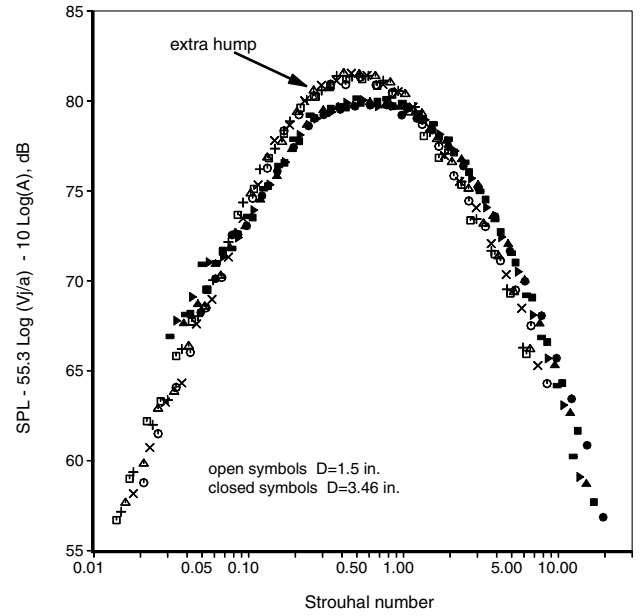

Fig. 21 Comparison of normalized spectra; $T_r/T_a = 3.2$, angle = 90 deg.

spectra for the larger nozzle ($D = 3.46$ in.), denoted by the closed symbols, collapse on to a different curve. The biggest difference between these two families of curves occurs near the spectral peak and at Strouhal numbers slightly lower than the peak, with the normalized levels being higher for the smaller jet. This trend, suggested here by Fig. 20 [and by Fig. 14 in [2] (with humps at all Mach numbers) and Fig. 15 in [2] (no such humps)], shows up clearly when the spectra are compared on a common basis. Thus, the observed change in spectral shape was unambiguously demonstrated to be an effect due to low Reynolds number. Further, it was proved that the overall power level does not exhibit a sixth-power dependence on velocity even at high jet temperatures. A critical value of the Reynolds number that would need to be maintained to avoid the effects associated with low Reynolds number was estimated to be $\sim 400,000$. The increase in noise levels and a shift in the peak frequency to lower values at high jet temperatures, noted in low Reynolds number experiments, have been attributed to the contribution from dipoles by many researchers. The results indicated that this hypothesis is erroneous and the observed increase in noise was due to the aforementioned scale effect and contamination by rig noise (see [2] for more details).

For the model-scale data used for comparison with engine data, it is made sure that the Reynolds number is above the threshold value so as to remove any effect of low Reynolds number on the spectra.

G. Effect of the State of the Flow at the Nozzle Exit

In addition to the Reynolds number, the state of the boundary layer at the nozzle exit plane could play a role in the comparison of model-scale data with engine data. Whereas the boundary layer in a model-scale nozzle could be laminar in many instances, the boundary layer in a jet engine is always turbulent. It has been traditionally believed that jets with a laminar boundary layer produce more noise than their turbulent counterparts, especially at the higher frequencies. Though the effect of the exit conditions on flow development has been studied extensively, there is limited information on their effect on noise. To understand the effect of the thickness and the state of the boundary layer upstream of the nozzle convergent (entrance) section and in the nozzle itself, Viswanathan and Clark [16] carried out a computational and experimental investigation. The main results of this study are summarized next.

Three nozzles of identical exit diameter, and hence the same Reynolds number for a given jet condition, were designed and tested. These three nozzles had a shallow conic section, a short cubic contraction, and an American Society of Mechanical Engineers (ASME) flowpath (contraction followed by a constant section), respectively. The internal contours of the nozzles were carefully shaped to control the thickness of the boundary layer. The internal lines of the conic and cubic nozzles, which represent the two extreme designs, are shown in Figs. 22a and 22b. The conical nozzle was originally designed to provide a uniform velocity profile over a range of nozzle pressure ratios. The use of a shallow cone angle (half-angle of 6.3 deg), although providing a uniform velocity, resulted in a long nozzle with substantial boundary-layer buildup. The contour of the cubic nozzle was made short and the surface curvature along the flow direction was smoothly decreased to zero at the nozzle exit. The main objective of the design was to accelerate the flow and minimize the thickness of the boundary layer.

Detailed flowfield analyses and measurements indicated that the boundary layers were laminar and turbulent for the cubic and conic nozzles, respectively. Figure 23 shows sample boundary-layer profiles at the nozzle exit plane for the two nozzles for a jet at a Mach number of 1.0 and temperature ratio of 2.7. The thickness of the boundary layer is defined as the distance at which the local velocity reaches 99% of the value in the core. As seen, the boundary layer is extremely thin for the cubic nozzle ($\sim$0.5 mm), whereas the thickness of the boundary layer for the conic nozzle is $\sim$7 mm. Figure 24 shows spectral comparisons from an unheated jet at a Mach number of 1.0 at three angles of 50, 90, and 145 deg for the two nozzles. These three angles cover a wide polar angular range; the first one is a low radiation angle, the second one is normal to the jet, and the third in the peak radiation sector. The spectral levels for the cubic and conic nozzles are virtually identical. Spectral comparisons are shown for a heated jet with a Mach number of 1.0 and a temperature ratio of 2.7 in Fig. 25. The spectral levels generated by the cubic nozzle are slightly higher than those for the conic nozzle, especially at 90 deg. However, even at 90 deg, the magnitude is only $\sim$1 dB. In the peak radiation sector in the aft angles, the peak levels are again nearly identical.

The important conclusion of this study is that the radiated noise is insensitive to the state of the flow and the thickness of the boundary layer at the nozzle exit plane, contrary to conventional belief. For more details, see [16]. Therefore, it should be possible to compare noise measurements from different facilities and different nozzle sizes.

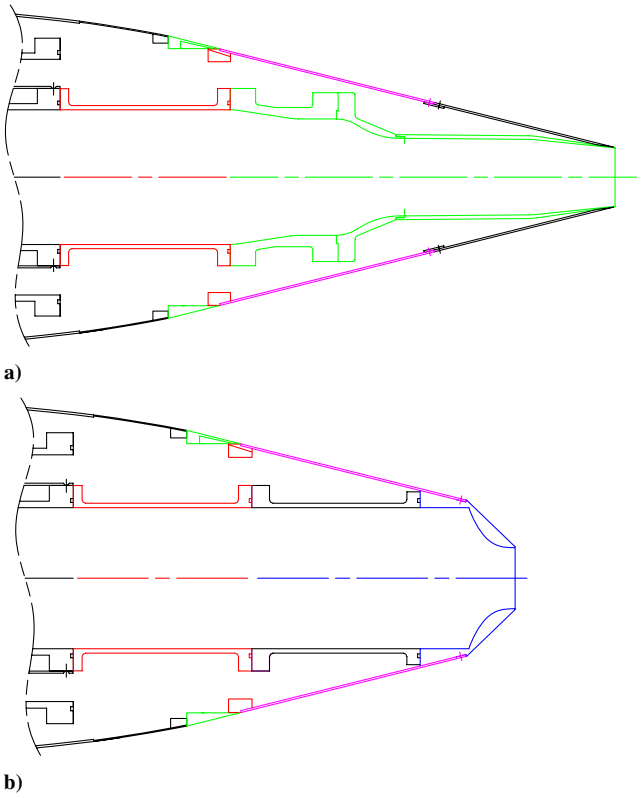

Fig. 22 Internal contours and flowpaths of the test nozzles: a) conic nozzle, b) cubic nozzle.

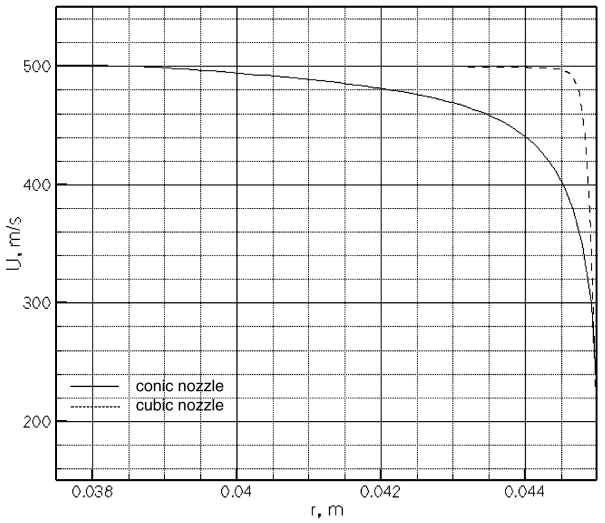

Fig. 23 Exit velocity profiles, $M = 1.0$, $T_r/T_a = 2.7$.

H. Concept of Perimeter Mixing

Many researchers have proposed in the past that by increasing the "shear perimeter" between the jet shear layer and the ambient fluid, it would be possible to increase mixing and reduce the radiated noise. This concept of perimeter mixing for noise reduction has been embraced by a few, especially in the context of multitube and multichute mixers. This issue has not been thoroughly investigated. Because there is an order of magnitude difference between the perimeter lengths for model nozzles and an engine, a simple test has been carried out here to verify the influence, if any, of the increased shear perimeter. A compound flow nozzle, the geometry of which corresponds to that of a low-bypass ratio mixed flow turbofan engine is considered. The trailing edge is modified with a chevronlike shape to increase the perimeter. Figure 26 shows the design, with the perimeter 96% longer than the corresponding baseline round nozzle.

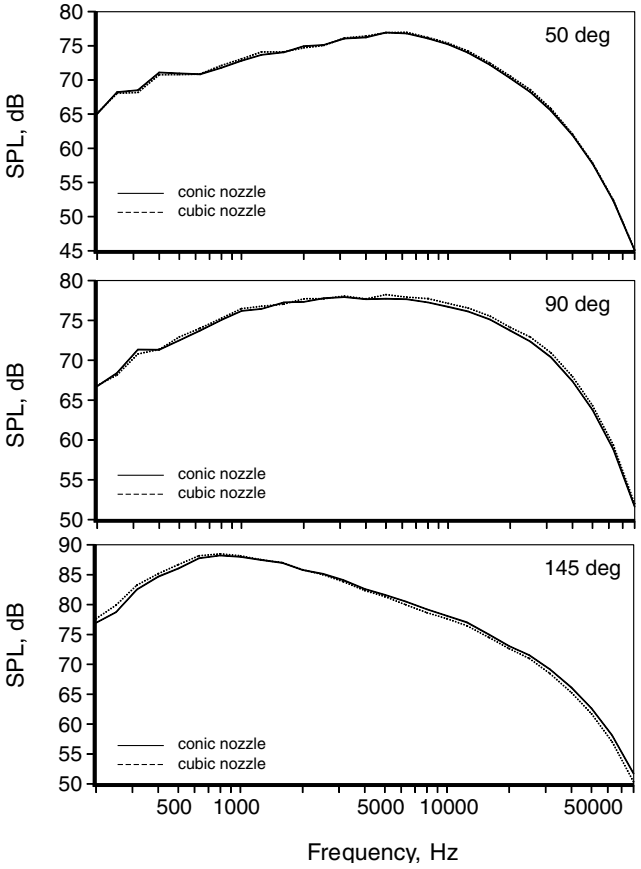

Fig. 24 Spectral comparisons, $M = 1.0$, $T_r/T_a = 1.0$.

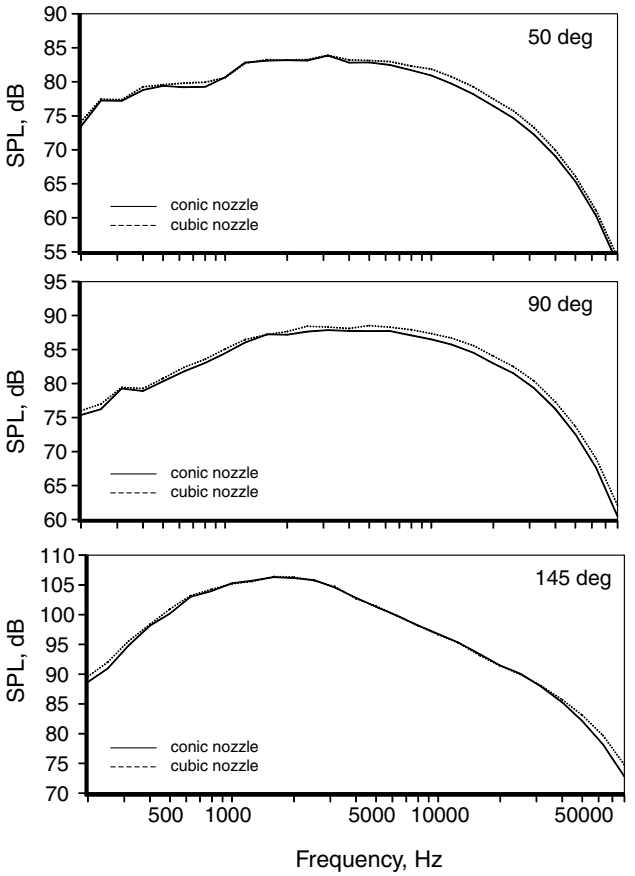

Fig. 25 Spectral comparisons, $M = 1.0$, $T_r/T_a = 2.7$.

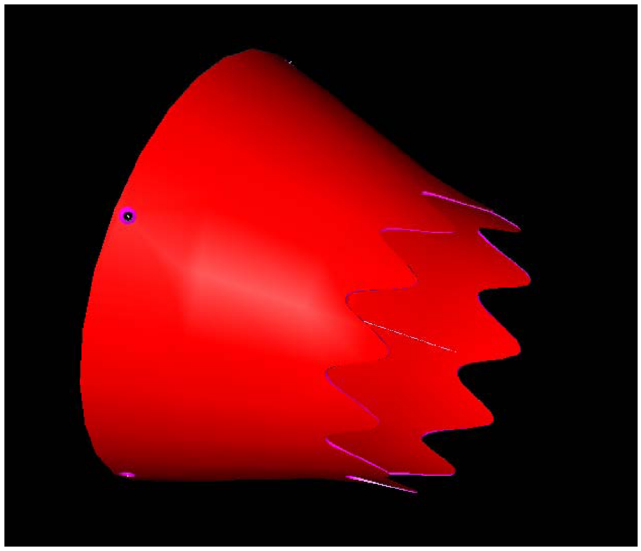

Fig. 26 Drawing of nozzle model with increased trailing-edge perimeter.

The chevrons are not immersed into the flow and hence may be regarded as "neutral chevrons."

Spectral comparisons between the baseline and modified nozzles are now presented. Figure 27 shows the measured spectra over a wide range of polar angles, with the operating conditions being subsonic, as follows: $\mathrm{NPR}_p = 1.57$, $T_p/T_a = 2.38$, $\mathrm{NPR}_s = 1.53$, $T_s/T_a = 1.18$. We see that the spectral levels are virtually identical over the entire frequency range at all angles. Similar agreement is seen at other subsonic conditions (not shown) as well. Next, we increase the NPR to supercritical values and establish shocks in the flow as follows: $\mathrm{NPR}_p = 2.63$, $T_p/T_a = 2.96$, $\mathrm{NPR}_s = 2.47$, $T_s/T_a = 1.23$. We anticipate that the shock-cell formation could be

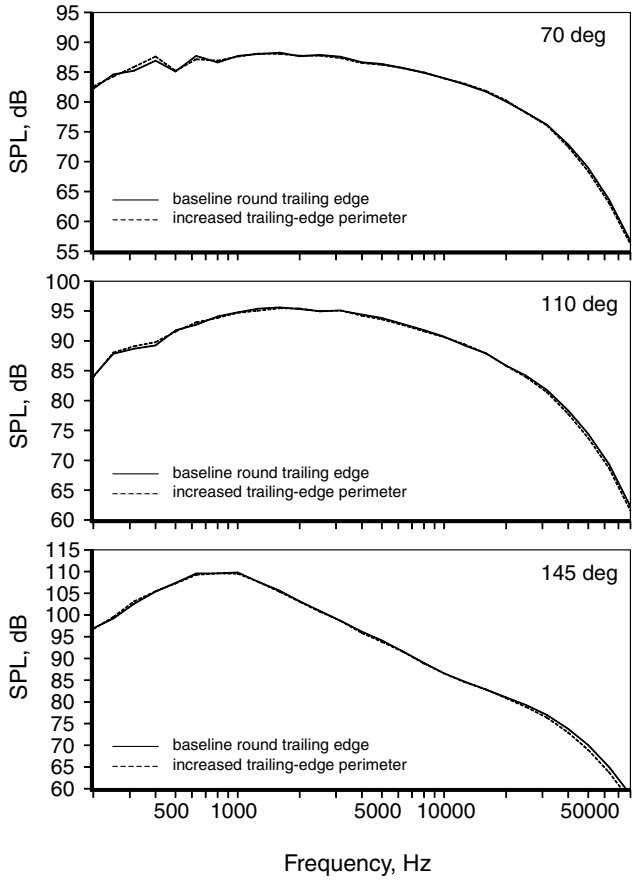

Fig. 27 Spectral comparisons from a compound flow nozzle, $Mt = 0.0$.

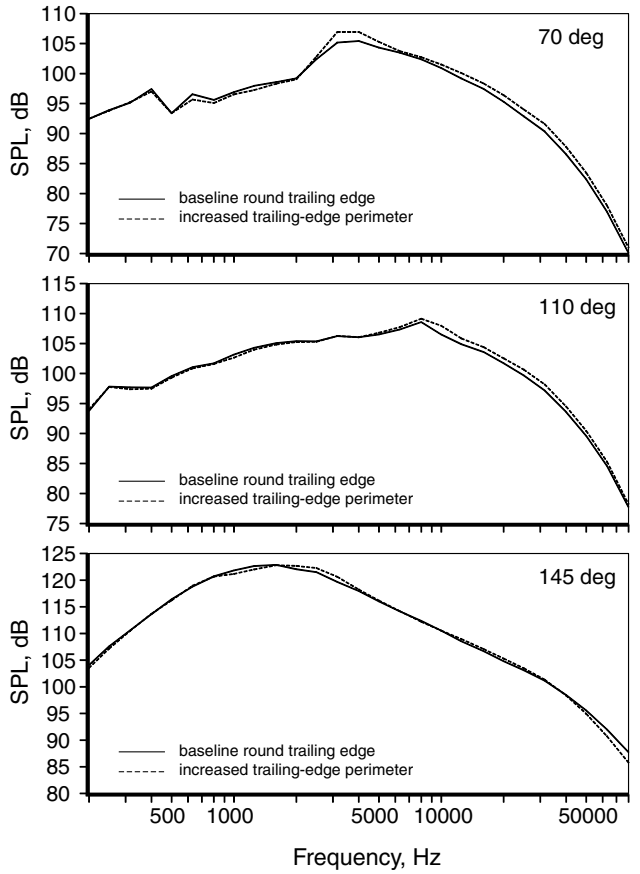

Fig. 28 Spectral comparisons from a compound flow nozzle, $Mt = 0.0$.

somewhat affected by the modified trailing edge. However, an examination of the spectra in Fig. 28 at various polar angles indicates only minor variations. The peak associated with the broadband shock-associated noise has slightly higher levels at 70 deg for the modified nozzle. As we move aft, the differences between the two sets of spectra decrease and the agreement is good over most of the frequencies. In the preceding two cases, there was no external stream. In Fig. 29, we present data at the same jet conditions as shown in Fig. 28, but with an external stream at a Mach number of 0.2. Again, the magnitude of the differences is comparable to those seen for the static case in Fig. 28. For the subsonic cases (not shown), the presence of a flight stream does not have any effect either. These trends are somewhat surprising because the spectral changes are very minor even at supercritical pressure ratios. It is fair to conclude then that increasing the shear perimeter, by roughly a factor of two, has no effect on jet noise. This observation should have been obvious from the results presented in Sec. III.E, where the flow area (and thrust) was used to normalize the spectra with excellent collapse demonstrated for several cases. Additional evidence is offered in Viswanathan [18]. Therefore, the vast disparity in the perimeter length between a model nozzle and an engine should have no impact on the comparisons.

I. Far Field for Jet Noise Measurements

The distributed nature of the noise sources in a jet requires particular consideration, both in the design of the measurement system and in the required distance of the microphones from the jet to avoid near-field effects. The various issues are examined in great detail in Secs. IV.C, IV.D, and IV.E in [3]. Here, a single issue, that of the minimum distance that must be maintained to be in the far field of a jet, is briefly reviewed. This is a pertinent issue, because the microphones in an engine test are usually placed on a polar arc of 150 ft (45.7 m) regardless of the engine size.

In the past, the near-field effects were quantified by moving a microphone progressively away or toward the jet and by examining

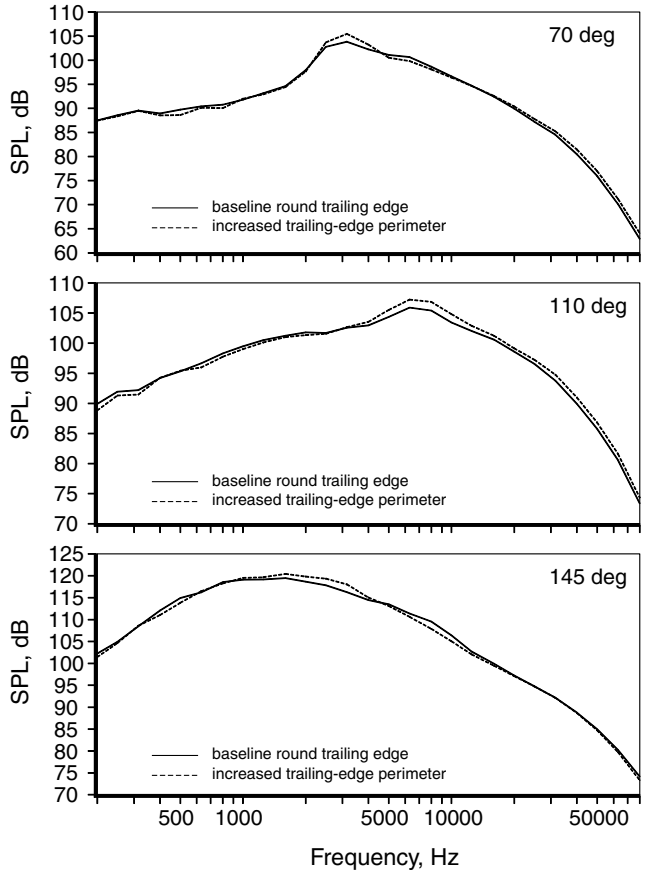

Fig. 29 Spectral comparisons from a compound flow nozzle, $Mt = 0.2$.

the spectral levels for $(1/r^2)$ dependence at every frequency. This method was adopted by Boeing and Lockheed in the early 1970s. The measured reduction in spectral level with distance is compared with the theoretical decay rate (6 dB reduction for a doubling of the distance) and the distance at which the two trends begin to deviate is designated as the limit of the near field. However, there is some subjectivity in how the comparison with the ideal decay rate is carried out. Therefore, a different approach was adopted in [3]. Spectra were measured from nozzles of increasing diameters with the same linear array of microphones, thereby progressively decreasing the nondimensional distance (r/D) to the microphones. The normalized spectra at the same jet conditions were compared to detect any near-field effects. Spectra from nozzles of different diameters of 1.5, 2.45, 3.46, 4.21, 4.71, and 4.9 in. at a fixed jet Mach number and temperature were normalized. A sample plot is included here as Fig. 30, for a $M = 1.0$ unheated jet at 90 deg. There is very good collapse of the data from the different nozzles throughout the frequency range. We observe the closest agreement at the lowest frequencies ($Sr \leq 0.4$). However, the magnitude of the scatter is only $\sim$1 dB even at the higher frequencies. The main conclusion is that there are no near-field effects at the lowest frequencies even for the larger nozzles. Additional evidence was offered in [3] with good agreement of data from a larger nozzle of 5.34-in.-diam $(r/D = 33.7)$ measured with microphones set at grazing and normal incidence (see Figs. 6–9 and associated discussion in [3]). Based on these results, it was concluded that a microphone distance of $\sim$35 D ensures measurements in the true acoustic and geometric far field for a jet and that no error is incurred with the assumption of a point source for greater microphone distances.

J. Comparison of Model Data with Engine Data

Finally, comparisons of scaled model data with engine data are presented. Many of the issues related to the scaling methodology, the choice of the method for calculating the atmospheric absorption coefficients, etc., have been addressed already. It is inherently better

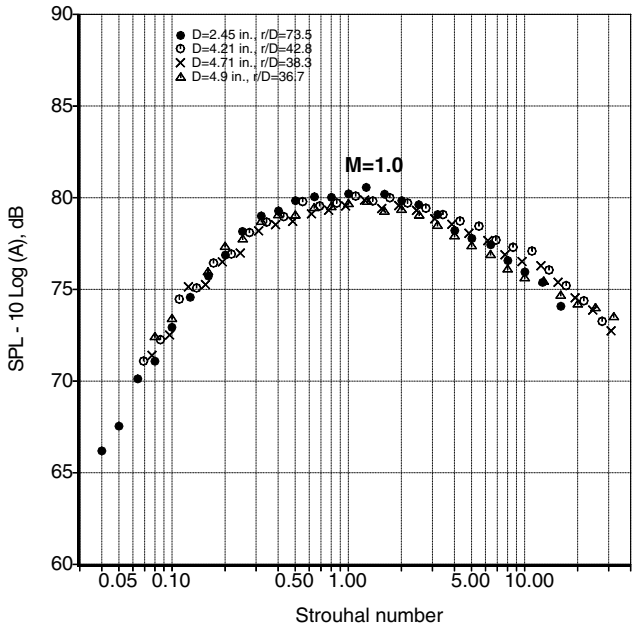

Fig. 30 Comparison of normalized spectra at 90 deg from an unheated jet. Microphone distance = 15 ft.

to locate the microphones in the far field and avoid the complications associated with source locations in the extrapolation/processing of data. Proprietary methods that account for source distributions are used by the aircraft industry. It has been ensured that the model-scale data have been acquired in the true far field. Therefore, the jet sources are assumed to be represented by a point source located at the center of the nozzle exit plane in the scaling of the model data shown next. The measured one-third-octave spectra in LSAF are first converted to lossless levels using the method of Shields and Bass [4] and the microphone distances from the assumed source position. The lossless spectra are then scaled and propagated to the measurement distances in an engine test. The atmospheric absorption coefficients given by the SAE method [7] are used for the engine scale frequencies.

Spectral comparisons over a wide range of polar angles and at four power settings of the static engine test described in Sec. II.A are presented in Figs. 31a, 31b, 32a, and 32b. Given the proprietary nature of the data, the absolute levels or the cycle conditions are not provided. Power levels 1–4 denote various conditions as follows: level 1 is the lowest, with a subsonic jet Mach number of 0.8; level 2 is at a transonic/slightly supersonic Mach number of 1.04; levels 3 and 4 are at supersonic Mach numbers of 1.23 and 1.43, with shocks established in the jet plume. To enhance the visual observation, spectra from power levels 1 and 3 are shown in Fig. 31, and power levels 2 and 4 in Fig. 32. The symbols denote the engine data and the lines denote the model data. First of all, we note that there is excellent agreement between the two sets of spectra at all the angles. There is clear demonstration that the good agreement is not confined to a few angles or a few power settings. Therefore, many conclusions may be drawn from these figures. The precautions taken to minimize the contribution from the other sources in the engine test have obviously led to the measurement of pure jet noise even at low polar angles, as evidenced by the good spectral match with the model data at all frequencies and at all power levels. There is also strong validation for the high quality and accuracy of the model data taken by the author (as reported in great detail in [1,2]). These comparisons also validate the scaling methodology adopted here and the recommended choices for the calculation of the coefficients of atmospheric absorptions at model and engine scales.

The humidity corrections in the frequency range of 50–80 kHz are in the range of 0.7–1.0 dB/ft, see Fig. 5a. At a polar angle of 150 deg, the microphone at LSAF is at a distance of 30 ft (9.14 m) from the center of the nozzle exit. Consequently, corrections of $\sim$20 to $\sim$30 dB are applied at the higher frequencies in converting

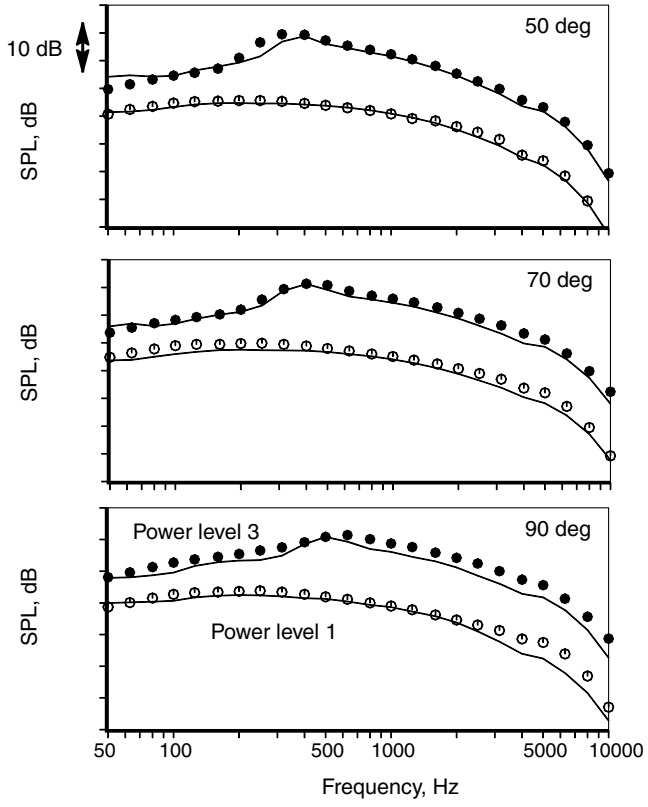

a)

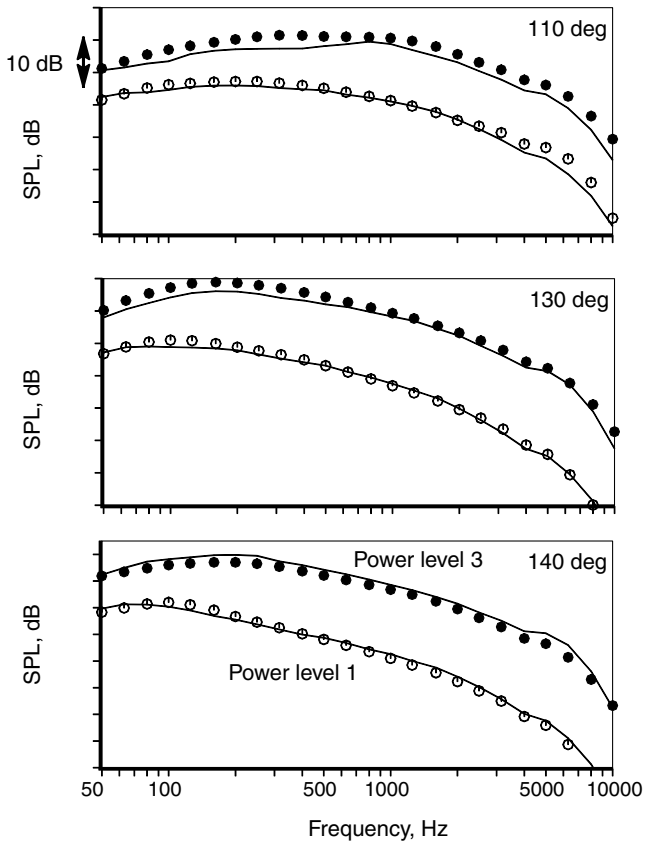

b)

Fig. 31 Comparison of model-scale data with engine data at power levels 1 and 3. Symbols indicate engine 1; lines indicate model scale.

the as-measured data to lossless form. The results shown in Figs. 8 and 10 (for the unheated jet) and the preceding comparisons of model and engine data indicate that the applied corrections are accurate. It is gratifying to note that the model-scale data at 80 kHz, when properly scaled and with the proper application of the microphone free-field

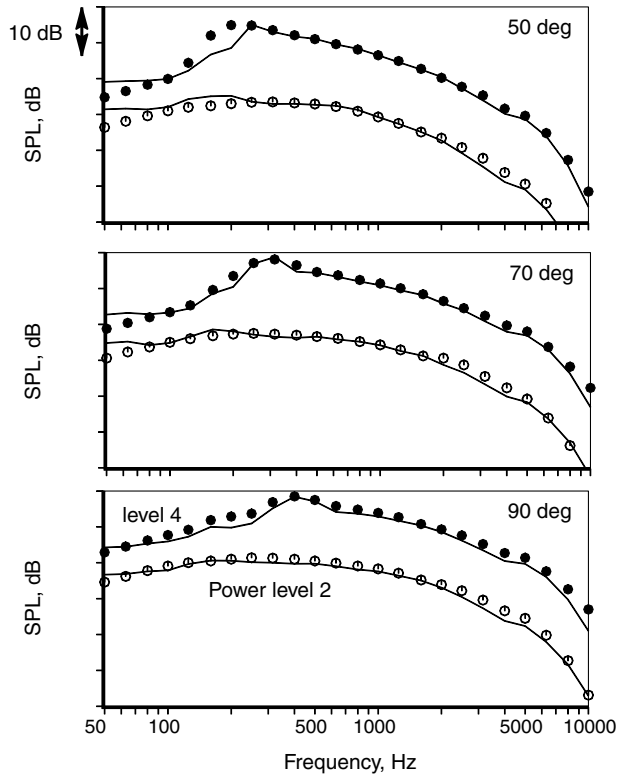

a)

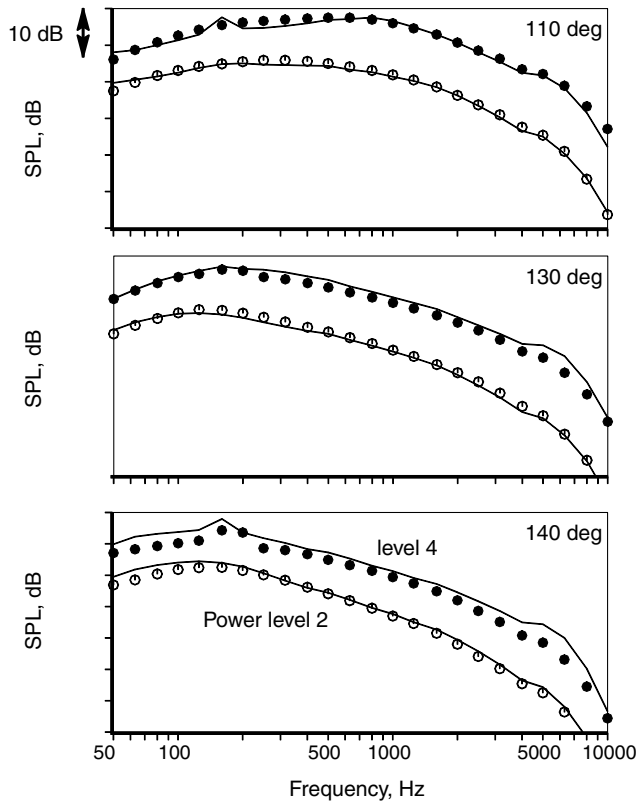

b)

Fig. 32 a. Comparison of model-scale data with engine data at power levels 2 and 4. Symbols indicate engine 1; lines indicate model scale.

and atmospheric corrections, indeed agree well with engine data at 10 kHz. Frequently, it is mentioned that there are uncertainties associated with the measurements at the higher frequencies because of the large corrections involved. First of all, the instrumentation system can be designed to minimize the magnitude of the microphone corrections (see Fig. 3a in [3]). Second, even if the atmospheric corrections are large, it does not necessarily mean that they are incorrect. It has been demonstrated unambiguously that it is possible to acquire accurate jet noise spectra up to 80 kHz. Much of the problems in the past measurements stem from severe contamination by rig noise, improper test planning and conduct, and to a lesser extent by the poor design of the instrumentation system, as described by Viswanathan [1–3]. As such, there is no inherent problem in making good spectral measurements up to 80 kHz given the state of the art in electronics and transducers, provided adequate care is taken. This is an important conclusion of this study.

Now, we present data from a second engine test, a "standard" test in which no special measures (such as the very long inlet duct or acoustically treated spool pieces) were taken to minimize the contribution from the nonjet sources. The total noise from the engine is therefore measured. This is a low-bypass ratio engine, operated at very high power. Figure 33 reveals that jet noise is the dominant component at this operating condition because there is fair agreement between the two sets of spectra. Again, there is good agreement at the higher frequencies attesting to the validity of the scaling process and the applied humidity corrections. Contrast the spectral shapes from these two engines to those from a high-BPR engine shown in Figs. 1–3. At lower powers (not shown) there is progressive worsening of the spectral match and, as expected, the turbomachinery noise begins to play a larger role in the total engine noise.

It has been proven here that model-scale jet noise data faithfully represent engine data. Therefore, the use of model data in the development of prediction methods and noise reduction devices is justified for full-scale applications. A low-BPR turbofan engine has been used in this study to demonstrate the preceding point. An additional factor must be considered when dealing with high-BPR turbofan engines. This issue pertains to the possible excitation of jet noise by the other components. Lu [24] carried out a careful study of this phenomenon with an extremely quiet blowdown jet rig at Boeing (see [1] for more details). He independently excited the primary or the secondary jet in a dual-stream nozzle and observed the following trends. For an exhaust geometry with an extended primary nozzle (a common configuration for high-BPR engines), the excitation of the secondary stream could produce excess jet noise, whereas the excitation of the primary stream leads to negligible noise increase. The magnitude of the noise increase is directly proportional to the strength of the excitation level; further, the magnitude of the excess noise is more pronounced at lower engine power settings. Excitation Strouhal numbers in the range of 0.5–0.6 are most effective in producing excess noise. The extrapolated data with excess noise agreed better with engine measurements, especially at low engine power and low polar angles. An examination of Fig. 2 indicates that the spikes at ~200 Hz are not captured by the prediction method based on clean data. The jet noise levels are usually adjusted in the engine noise model at these frequencies, unless a tone generated by the turbomachinery can be explicitly identified at this frequency, such that the extracted levels of jet noise match the engine data (the adjusted curve is not shown here to specifically illustrate that minor tweaks are needed to match engine data).

Therefore, the model-scale jet noise for high-BPR turbofan engines should also represent the jet noise from turbofan engines, once we recognize the possible effect of the excitation of the fan stream and account for it. In most cases, this step involves adjusting the jet noise spectra to include the tones observed at the lower frequencies from jet engines. Much of the confusion prevailing about the excitability (or lack thereof) of jets is due to contaminated data obtained in most facilities. As noted in [1], these jets were unwittingly excited in these facilities by rig noise, consequently masking the true effect of an imposed excitation as was done in a clean facility by Lu [24]. Based on the preceding measurements, Lu

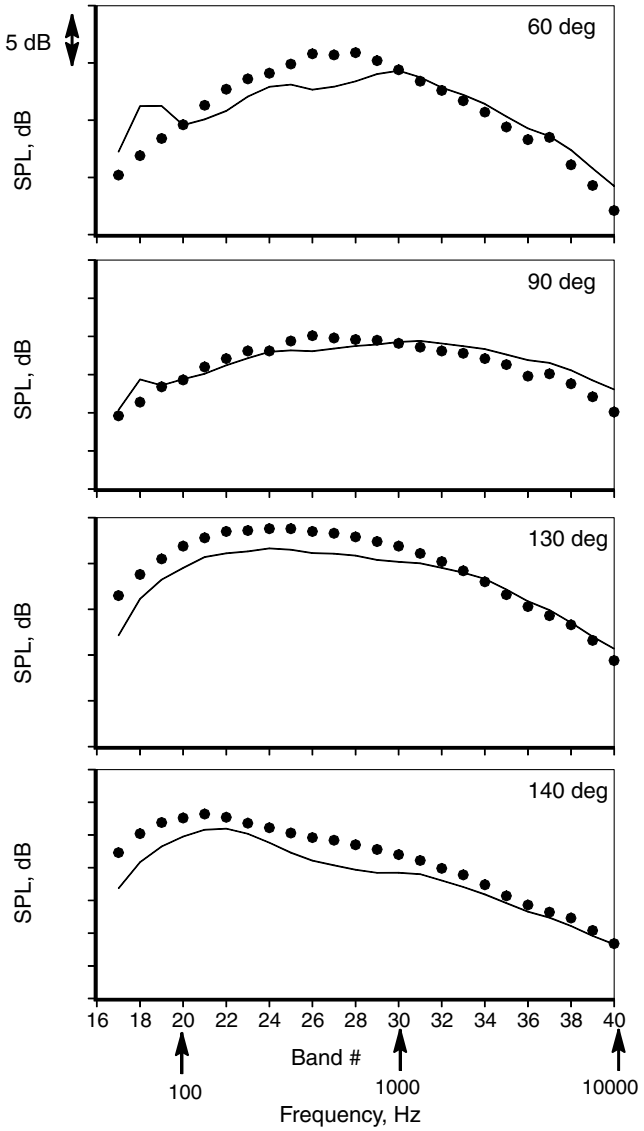

Fig. 33 Comparison of model-scale data with engine data at high power. Symbols indicate engine 2; lines indicate model scale.

[25] developed empirical adjustments that include the effects of the excitation of the fan jet in the prediction method for jet noise. The method of [25] was adopted by the SAE committee as the preferred method for jet noise prediction from high-BPR turbofan engines (see [26]) and is used widely by the industry. Finally, a prediction method, most probably empirical in nature, based on high-quality model data should aid in the identification of jet noise spectra from high-BPR turbofan engines with multiple noise sources. Once again, it is reiterated that every effort should be made to acquire high-quality noise spectra in scale-model nozzle tests, as this is a critical and vital component for improving jet noise technology.

IV. Conclusions

A thorough experimental study has been carried out to verify whether a model-scale nozzle produces the same jet noise as a jet engine, with the twin goals of 1) validating the practice of carrying out jet noise research at model scale for full-scale applications, and 2) aiding the identification of jet noise in measured total spectra from jet engines. Many issues that are pertinent in permitting the comparison of scaled model data with engine data have been investigated. The salient conclusions from the test programs and analyses are enumerated as follows:

1) For aircraft application, accurate spectral measurements are necessary at all frequencies and at all angles. The instrumentation

requirements for model-scale tests, where spectral information is needed at high frequencies (typically up to 80 kHz), are more stringent. Care is needed in designing the instrumentation system, so as not to compromise the measurements at the higher frequencies. A good practice is to orient the microphone at normal incidence and point it at the nozzle exit in model tests (see [3] for complete details). Even though the microphones are set at grazing incidence in engine tests, the application of the appropriate corrections yield identical spectra regardless of the microphone orientation.

2) Three available methods for the calculation of the atmospheric attenuation coefficients have been examined; the coefficients given by these methods are different at the higher frequencies. Spectral measurements with four microphones at different distances (r/D) were made at various jet velocities. These spectra were then collapsed assuming spherical divergence of the pressure ($1/r^2$ dependence); the application of the absorption coefficients due to Shields and Bass [4] produces excellent collapse of the data over the entire frequency range. The atmospheric corrections applied to either the narrowband or one-third-octave spectra yield the same end result.

3) This exercise was also used to examine the propagation characteristics, linear and nonlinear, of acoustic waves at different jet velocities and sound amplitudes. First of all, nonlinear propagation occurs even for subsonic heated jets in laboratory measurements. To demarcate the threshold jet velocity above which nonlinear propagation effects are observed, the normalized spectra at two microphone distances for progressively increasing jet velocities were examined. Nonlinear effects manifest themselves when the convective Mach number of the jet becomes supersonic, a result established for the first time. The jet velocity that corresponds to this condition is $\sim$1600 ft/s (490 m/s). It is proposed here that the convective Mach number is a good indicator of nonlinear propagation for jet noise, rather than the high absolute amplitudes of the sound as has been believed in the past. A methodology for handling this phenomenon is necessary. Detailed flow measurements that would shed light on this phenomenon are underway; the results will be published in the future.

4) A set of high-quality benchmark data have been acquired in a controlled anechoic environment that would help the development and refinement of prediction methods for acoustic wave propagation. These data are at jet velocities that lead to both linear and nonlinear propagation.

5) With proper care, highly repeatable and consistent spectra, with a scatter range of $\pm$0.25 dB at all frequencies (see [3]) can be acquired. It is important not to confuse repeatability with accuracy. However, if there is wide scatter in the data from repeat runs, the situation is hopeless, especially in the evaluation of noise reduction concepts.

6) The steps involved in the scaling of jet noise spectra have been reviewed in depth. With proper scaling factors for nozzle area and velocity, good collapse of both narrowband and one-third-octave spectra are achieved, both for turbulent mixing noise and broadband shock-associated noise. The velocity dependence of OASPL depends on the radiation angle and jet temperature. The use of the Doppler factor for normalizing the frequency, especially in the aft quadrant, leads to poor spectral collapse and hence should be rejected. Based on the results, new scaling laws have been developed in [18]; master spectral shapes have been generated at all radiation angles and for a variety of jet temperature ratios. A practical and accurate prediction method based on the new scaling laws is presented in [21].

7) As summarized here (see [2] for details), there is a change in spectral shape at the lower polar angles for highly heated subsonic jets. This change is due to effects associated with low Reynolds number. These effects have been avoided in the current model tests.

8) The state of the boundary layer at the nozzle exit plane could be laminar in model tests, whereas it is turbulent in an engine. Sample spectral measurements provided indicate that the radiated noise is insensitive to the state and thickness of the boundary layer at the nozzle exit plane (see [16] for details). Therefore, it is established that the state of the boundary layer would have no impact on model-engine noise comparisons.

9) The concept of perimeter mixing was investigated by increasing the perimeter length with a nonimmersed chevron shape of the nozzle trailing edge. Surprisingly, a doubling of the shear perimeter was seen to have virtually no effect on noise. This was so even at supercritical NPR, where one would expect the shock formation, and hence the shock-associated noise, to be altered by the local conditions at the nozzle trailing edge. This result leads to the conclusion that even though the perimeter lengths are an order of magnitude different between the engine and the model nozzle, there would be no effect on noise comparisons.

10) The distance that represents the true far field for jet noise measurements was established in [3]. A sample result presented here indicates that a distance of $\sim$35 D ensures measurements in the far field of distributed jet noise sources.

11) A special test was carried out to measure pure jet noise at all angles from a jet engine. Model-scale spectra were scaled to engine scale using the procedure described earlier. The atmospheric attenuation corrections at model scale were obtained by the method of Shields and Bass [4] and at engine scale by the SAE method [7]. Excellent agreement between the two sets of spectra was demonstrated at all angles and frequencies for many power settings. Conclusive evidence that model data faithfully reproduce engine data is presented.

12) It is possible to acquire high-quality spectra up to 80 kHz in model tests, provided proper steps are taken in planning the test and in designing the instrumentation system.

13) Atmospheric attenuation corrections are quite accurate even at the higher frequencies of interest at model scale (up to 80 kHz) and the procedure recommended here is valid for engineering applications.

Acknowledgments

It is a pleasure to thank many of my friends and colleagues (too numerous to name individually) from NASA Langley and NASA John H. Glenn Research Centers, General Electric Aircraft Engines, Pratt and Whitney, and Boeing in the High-Speed Research/High-Speed Civil Transport Program who were involved in the static engine test. Technical discussions with these colleagues were valuable in the research and the results presented here.

References

[1] Viswanathan, K., "Jet Aeroacoustic Testing: Issues and Implications," *AIAA Journal*, Vol. 41, No. 9, 2003, pp. 1674–1689.

[2] Viswanathan, K., "Aeroacoustics of Hot Jets," *Journal of Fluid Mechanics*, Vol. 516, Oct. 2004, pp. 39–82. doi:10.1017/S0022112004000151

[3] Viswanathan, K., "Instrumentation Considerations for Accurate Jet Noise Measurements," *AIAA Journal*, Vol. 44, No. 6, 2006, pp. 1137–1149.

[4] Shields, F. D., and Bass, H. E., "Atmospheric Absorption of High Frequency Noise and Application to Fractional-Octave Band," NASA CR 2760, June 1977.

[5] Anon., "Condenser Microphones and Microphone Preamplifiers for Acoustic Measurements," *Brüel and Kjaer Handbook*, Naerum, Denmark, Sept. 1982.

[6] Anon., "American National Standard Method for the Calculation of the Absorption of Sound by the Atmosphere," American National Standards Inst., ANSI S1.26-1978, New York, revised in 1986.

[7] Anon., Aerospace Recommended Practice, Society of Automotive Engineers, SAE ARP866A,15 March 1975.

[8] Viswanathan, K., "Analysis of the Two Similarity Components of Turbulent Mixing Noise," *AIAA Journal*, Vol. 40, No. 9, 2002, pp. 1735–1744.

[9] Pestorius, F. M., and Blackstock, D. T., "Propagation of Finite Amplitude Noise," *Finite Amplitude Wave Effects in Fluids*, edited by L. Bjørnø, IPC Science and Technology Press, England, U.K., 1974, pp. 24–29.

[10] Blackstock, D. T., "Nonlinear Propagation Distortion of Jet Noise," *Proceedings, Third Interagency Symposium on University Research in Transport Noise*, Univ. of Utah, Salt Lake City, UT, Nov. 1975, pp. 389–397.

[11] Crighton, D. G., and Bashforth, S., "Nonlinear Propagation of Broadband Jet Noise," *AIAA 6th Aeroacoustics Conference*, AIAA Paper 80-1039, 1980.
[12] Gallagher, J. A., and McLaughlin, D. K., "Experiments on the Nonlinear Characteristics of Noise Propagation from Low and Moderate Reynolds Number Supersonic Jets," *7th Aeroacoustics Conference*, AIAA Paper 81-2041, 1981.
[13] Howell, G. P., and Morfey, C. L., "Nonlinear Propagation of Broadband Noise Signals," *Journal of Sound and Vibration*, Vol. 114, No. 2, 1987, pp. 189–201.
doi:10.1016/S0022-460X(87)80147-5
[14] Gurbatov, S. N., Malakhov, A., and Saichev, A., "Nonlinear Random Wave and Turbulence," *Nondispersive Media: Waves, Rays, and Particles*, Manchester Univ. Press, Manchester, England, U.K., 1991.
[15] Petitjean, B. P., Viswanathan, K., and McLaughlin, D. K., "Acoustic Pressure Waveforms Measured in High Speed Jet Noise Experiencing Nonlinear Propagation," *International Journal of Aeroacoustics*, Vol. 5, No. 2, 2006, pp. 193–215.
doi:10.1260/147547206777629835
[16] Viswanathan, K., and Clark, L. T., "Effect of Nozzle Internal Contour on Jet Aeroacoustics," *International Journal of Aeroacoustics*, Vol. 3, No. 2, 2004, pp. 103–135.
doi:10.1260/1475472041494819
[17] Gaeta, R. J., and Ahuja, K. K., "Subtle Differences in Jet-Noise Scaling with Narrowband Spectra Compared to 1/3-Octave Band," AIAA Paper 2003-3124, May 2003.
[18] Viswanathan, K., "Scaling Laws and a Method for Identifying Components of Jet Noise," *AIAA Journal*, Vol. 44, No. 10, 2006, pp. 2274–2285.
doi:10.2514/1.18486
[19] Lush, P. A., "Measurements of Subsonic Jet Noise and Comparison with Theory," *Journal of Fluid Mechanics*, Vol. 46, No. 3, 1971, pp. 477–500.
doi:10.1017/S002211207100065X
[20] Lighthill, M. J., "On Sound Generated Aerodynamically, 1: General Theory," *Proceedings of the Royal Society of London, Series A: Mathematical and Physical Sciences*, Vol. 211, 1952, pp. 564–581.
[21] Viswanathan, K., "Improved Method for Prediction of Noise from Single Jets," *AIAA Journal*, Vol. 45, No. 1, 2007, pp. 151–161.
doi:10.2514/1.23202
[22] Seiner, J. M., "Advances in High Speed Jet Aeroacoustics," AIAA Paper 84-2275, Oct. 1984.
[23] Tam, C. K. W., Golebiowski, M., and Seiner, J. M., "On the Two Components of Turbulent Mixing Noise from Supersonic Jets," AIAA Paper 96-1716, May 1996.
[24] Lu, H. Y., "Effect of Excitation on Coaxial Jet Noise," *AIAA Journal*, Vol. 21, No. 2, 1983, pp. 214–220.
[25] Lu, H. Y., "An Empirical Model for Prediction of Coaxial Jet Noise in Ambient Flow," AIAA Paper 86-1912, July 1986.
[26] Anon., "Gas Turbine Jet Exhaust Noise Prediction," Society of Automotive Engineers, SAE ARP876, Revision D, 1994.

K. Ghia
Associate Editor